Response of high-temperature superconductors to electromagnetic radiation: (A Review)

A. V. Velichko and N. T. Cherpak

Citation: Low Temperature Physics **24**, 297 (1998); doi: 10.1063/1.593592
View online: http://dx.doi.org/10.1063/1.593592
View Table of Contents: http://scitation.aip.org/content/aip/journal/ltp/24/5?ver=pdfcov
Published by the AIP Publishing

Response of high-temperature superconductors to electromagnetic radiation: (A Review)

A. V. Velichko and N. T. Cherpak

*A. Usikov Institute of Radiophysics and Electronics, National Academy of Sciences of the Ukraine, 310085, Kharkov, Ukraine**

(Submitted May 15, 1997; revised January 5, 1998)
Fiz. Nizk. Temp. **24**, 395–428 (May 1998)

Nonequilibrium processes resulting from the interaction of high-temperature superconductors with electromagnetic radiation are considered from microwave to optical range. Emphasis is laid on the dependence of surface or dc resistance on external parameters (temperature, bias current, modulation frequency, magnetic field, radiation power, and frequency), which is characteristic of every nonbolometric response mechanism considered by us. The most frequently used methods for monitoring the response of HTSC to electromagnetic radiation are described. © *1998 American Institute of Physics.* [S1063-777X(98)00105-4]

INTRODUCTION

A high superconducting transition temperature T_c (>77.3 K) together with a small coherence length ξ and a strong anisotropy are responsible for diverse and unusual electromagnetic properties of HTSC as compared to conventional superconductors. Among other things, the concept of vortex lattice and of the shape and dynamics of the vortices themselves have been revised significantly (see, for example, the review by Blatter *et al.*[1]) The transformation of magnetic vortices and the peculiarities of their mutual interaction associated with a strong anisotropy and fluctuational effects have led to various phase transitions and new states of the vortex lattice, e.g., lattice fusion, thermally induced depinning, collective flux creep, and $2D-3D$ transition. All these peculiarities call for a detailed and thorough analysis of the electromagnetic properties of HTSC which is interesting not only from a scientific, but also from a technical point of view.[2] For example, one of the most important and relatively simple applications of HTSC is the development of electromagnetic radiation (EMR) detectors. A negligibly small dispersion (for frequencies $\nu \ll 2\Delta/\hbar$, 2Δ being the band gap in the quasiparticle spectrum), steepness of the HTSC transition, and the use of a cheap coolant (liquid nitrogen) urged scientists to explore the possibility of creating HTSC bolometers working at liquid nitrogen temperature.[3,4] The main drawback of such devices is that a compromise has to be sought between sensitivity and high-speed response. Hence it is preferable to use nonbolometric detectors. In this connection, the study of nonequilibrium mechanisms for monitoring the response of HTSC to EMR assumes a special significance. By response we mean the variation of a certain characteristic of the material under the effect of an external agency (in the present work, we shall take for such a characteristic the resistance R of the sample exposed to EMR).

In the general form, the response mechanisms can be divided into two large groups covering bolometric (equilibrium) and nonbolometric (nonequilibrium) response. The bolometric mechanism is one of the most thoroughly investigated mechanisms[4] and hence we shall not consider it in the present work.

In recent publications devoted to the study of optical response[5–8] of microbridges made of epitaxial YBaCuO films, it is assumed that nonbolometric mechanisms are realized not only in granular samples, but also in high-quality HTSC. However, the controversy in the observed values of sensitivity and response time for the same nonthermal mechanisms has not been resolved so far. Most probably, it is linked not with the intrinsic properties of HTSC, but with various external conditions (temperature, bias current, magnetic field, radiation power, wavelength, pulse duration, etc.) under which these characteristics are obtained.[9] In this connection, it is necessary to study nonbolometric mechanisms in samples of the same quality under identical external conditions, and to investigate the conditions for optimizing the characteristics of detectors.

In this communication, we present a review of the most typical results on the investigation of nonequilibrium mechanisms of the response of HTSC to EMR, and systematize the existing mechanisms from the point of view of the most general physical effects characterizing superconductors. We shall not consider in this review the results of investigations in the fields of Raman scattering, generation of harmonics of the fundamental signal, photoluminescence, etc.

The review consists of the following parts. Typical methods for monitoring the response to EMR from the microwave (MW) to optical range are described in Sec. 1. Section 2 is devoted to a review of experimental works on the nonbolometric response mechanisms in HTSC, and to their classification into subgroups. The main results obtained in this field are summarized at the end of the review.

1. METHODS OF RESPONSE MONITORING

In response monitoring, it is important to take into consideration the frequency of the incident radiation and the technique used for monitoring. The former determines the processes induced by the incident radiation, and the latter

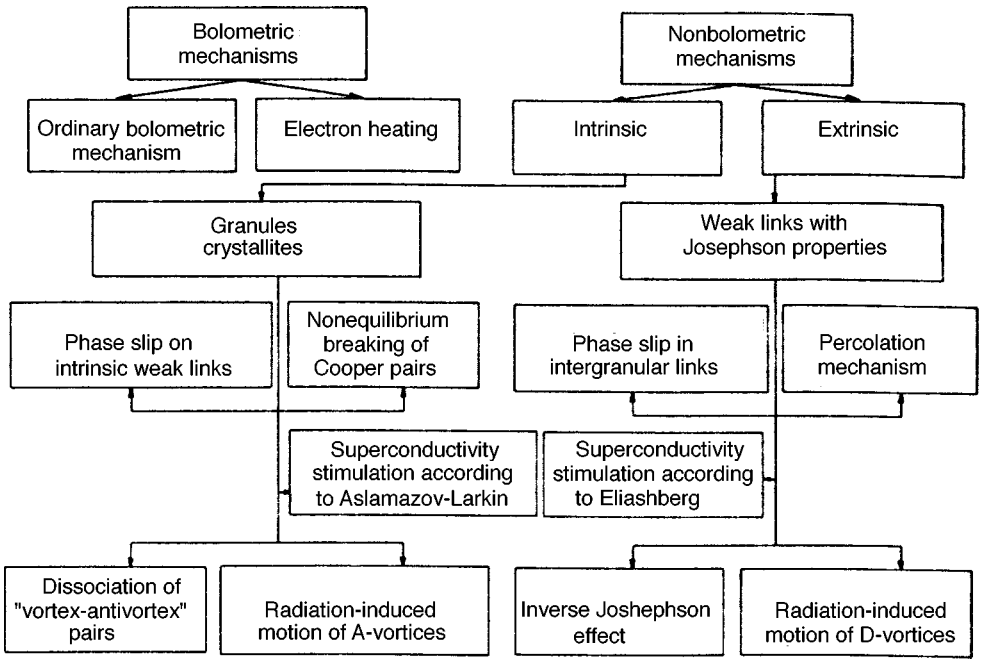

FIG. 1. Mechanisms of electromagnetic radiation monitoring by superconductors.

indicates the processes that may be discovered. The response is conventionally measured in direct current. In spite of the high sensitivity associated with the steepness of the superconducting transition in dc measurements, this method has a number of significant drawbacks. In the first place, special restrictions are imposed on the sample geometry: the thickness of the HTSC film must be smaller than or of the order of the radiation penetration depth δ. Otherwise, a part of the sample in which the radiation does not penetrate will shunt the layer whose properties have changed under exposure, and no response will be detected. Moreover, since the dc resistance of the sample in the superconducting state is equal to zero, the HTSC sample has to be processed with a view toward creating an element with nonzero resistance. In turn, this restricts the range of mechanisms available for monitoring the response. Besides, significant constraints on the noise characteristics of HTSC detectors are imposed by contact resistances of the order of 1 Ω, which are inescapable in such a detection technique.[10] These drawbacks are eliminated in the rf-technique for monitoring the response, although the sensitivity may decrease in this case due to a less steep superconducting transition and a smaller drop in the rf resistance as compared with the dc resistance. The rf-technique used by us for the first time[11] to monitor the response is based on the inductive technique[12] at radiofrequencies (rf) as well as the resonant technique[13] for measuring the MW response. Obviously, the problems associated with fluctuational noise and the degradation of the HTSC element due to contact phenomena are eliminated during rf monitoring of the response. Moreover, the constraints on sample thickness are less stringent in this case, since the only requirement is the overlapping of the incident radiation and the probing radiation penetration regions. Finally, the rf-technique for monitoring the response allows the detection of nonequilibrium processes even in the superconducting transition region, while a large value of the contact resistance and strong nonlinear effects associated with a constant measuring current lead to thermal instability and an ''avalanche''-type crossover to the bolometric regime.

Another effective method of studying the optical response of HTSC is the pump-probe technique[14,15] based on the use of the same agency (usually, a laser) as the source of radiation incident on the sample, and for monitoring the response by measuring the reflectivity of the probing signal. In this case, the nonequilibrium processes can be monitored over a wide range of wavelengths (from 10 μm to ultraviolet). The measuring signal is usually much weaker and is delayed relative to the pumping signal. The resolving power of such a technique is determined by the minimum possible duration of the laser pulse. For an optimal construction of the sensitive element, the amplitude of the nonthermal component is higher than the amplitude of the bolometric component at $T>80$ K by an order of magnitude.[6]

2. CLASSIFICATION OF RESPONSE MECHANISMS

We are not aware of any classification for the mechanisms of HTSC response to EMR showing their mutual relation with the most typical physical phenomena in superconductors. Such a classification is essential for a proper understanding of the processes stimulated in HTSC by the incident radiation. We believe that, while speaking of nonequilibrium response mechanisms, we must indicate clearly whether a particular mechanism is a property of the given sample or a common feature of the entire class of HTSC. In this respect, all nonbolometric response mechanisms can be divided into two groups, viz., intrinsic and extrinsic (see block diagram in Fig. 1). The intrinsic properties of HTSC are determined by the quality of single crystals and granules (for granular samples). At present, it is assumed that weak links between granules act as a chain of series- and parallel-connected Josephson junctions (JJ) responding synchro-

nously to the incident radiation. Hence the extrinsic properties of HTSC are mainly determined by the properties of a solitary JJ. Apparently, the intrinsic properties of HTSC are mainly similar to the properties of low-temperature type II superconductors with some differences associated with the peculiarities of the HTSC structure. Each of the above-mentioned large categories contains several mechanisms that are common to both groups.

2.1. Radiation-induced creep and flow of magnetic flux

The idea of thermally induced creep was put forth by Anderson,[16] while Zel'dov *et al.*[17] and Frenkel *et al.*[18] were among the first to detect the motion of magnetic flux induced in HTSC by radiation. Zel'dov *et al.*[17] studied the response of microbridges made of epitaxial YBaCuO films on $LaGaO_3$ and $SrTiO_3$ substrates to optical radiation (He–Ne laser, wavelength $\Lambda = 633$ nm), and found that the peak on the temperature dependence of the response is displaced by several degrees towards lower temperatures relative to the dR/dT peak characterizing the bolometric response. They also noticed a significant suppression of the response ΔR with increasing bias current, which was not observed in the temperature dependence of dR/dT. Moreover, the quantity $\Delta R/(dR/dT)$ characterizing the heating of the film in a purely bolometric effect increases sharply and has a peak at a temperature slightly lower than the superconducting transition temperature T_c. Since the thermal properties of the substrate, film, or the interface between them should not vary significantly in this temperature range, the authors concluded that the response is of nonbolometric type. Considering a strong correlation between the behavior of transport properties upon irradiation and without radiation, Zel'dov *et al.*[17] interpreted their results as magnetic flux creep induced by optical radiation. A similar interpretation of the results on the measurement of optical response was given by Frenkel *et al.*[18] who reported the observation of photo-induced depinning of magnetic flux. According to Frenkel,[19] the necessary condition for the emergence of flux flow is that the radiation quantum energy $h\nu$ must exceed the activation energy U_0 of the vortex lattice. The author believes that the photon energy is transferred thermally to flux lines, although other mechanisms of energy transfer (for example, the Lorentz force exerted on a vortex by the induced current) cannot be ruled out.

Eideloth[20] observed the response of BiSrCaCuO ceramic bridges and a meander made of epitaxial YBaCuO film on MgO substrate to optical radiation of wavelength $\Lambda = 633$ nm and concluded that his results can also be explained by the model of the photo-induced flux flow (PIFF). Moreover, the results of measurement on the BiSrCaCuO samples are described correctly by the PIFF model as well as the model of JJ network in which phase slip centers (PSC) are formed under the action of light as a vortex moves through the junction. It was also observed[20] that since the value of U_0 in the PIFF model and the energy barrier $2E_c$ in the JJ network model are close, these two mechanisms can be distinguished only by measuring the temperature dependence of the activation energy.

The contribution to the dc resistivity made by thermally activated flux creep in the case of a linear current–voltage characteristic (IVC) of the sample is described by the expression (see, for example, Ref. 21)

$$\rho = \frac{2\nu_0 \Phi_0^2 L_c}{k_B T} \exp(-U_0/k_B T), \tag{1}$$

where ν_0 is the attempt frequency, i.e., characteristic frequency of attempts by vortices to break away from the pinning center ($\sim 10^{12}$ Hz for YBaCuO single crystals), Φ_0 is the magnetic flux quantum, L_c is the coherence length along a flux line or a vortex bundle (which may vary from fractions of d for very thin samples to d for thick samples, d being the film thickness), and the energy $U_0 \sim 2 \cdot 10^5$ K for YBaCuO single crystals at $T \ll T_c$.[21] As a result, we obtain for the pre-exponential factor in formula (1) $\rho_0 = 10^5$ $\mu\Omega \cdot$cm. Note that formula (1) is in good agreement with the experiment for $\rho < 10^{-2}\rho_n$, where ρ_n is the resistivity in the normal state. For $\rho > 10^{-2}\rho_n$, an excellent agreement is obtained with Tinkham's theory[22] in which it is assumed that resistance, which is associated with flux creep, depends on U_0 in the same way as in the case of dissipation due to thermally induced phase slip in a JJ suppressed strongly by the transport current. According to the Ambegaokar-Halperin theory,[23] the JJ resistance in a strongly suppressed state has the form

$$\rho/\rho_n = [I_0(\gamma_0/2)]^{-2}, \tag{2}$$

where I_0 is the modified Bessel function, and $\gamma_0 = U_0/k_B T$. The following dependence on temperature and magnetic field H is proposed for U_0:

$$U_0 \propto \frac{(1 - T/T_c)^{3/2}}{H}. \tag{3}$$

Palstra *et al.*[21] reported that the dependence (3) is valid only over a limited temperature range, and a different temperature- and magnetic field dependence for U_0 obtained, for example, in the vortex glass model[24,25] or the thermally activated flow model,[26] cannot be ruled out.

If the Lorentz force F_L exerted on vortices by the transport current flowing through the sample is such that they acquire an energy $U_L = U_0$, depinning of vortices and a transition to the flux flow regime take place.[27] According to the Bardeen–Stefan theory,[27] the flux flow resistance is described by the expression

$$\rho_{ff} = \rho_n H/H_{c2}, \tag{4}$$

where H_{c2} is the upper critical field.

As regards the rf response associated with the flux flow, it was shown by Ji *et al.*[28] that at temperatures not very close to T_c and for $h\nu \ll 2\Delta$, the specific impedance taking into account the contribution from flux flow can be presented in the form

$$\rho = \frac{\Phi_0 B_{\text{eff}}}{\eta c^2} + \frac{4\pi\omega\lambda_L^2}{c^2}, \tag{5}$$

where η is the viscosity, $\omega = 2\pi\nu$ the angular frequency, λ_L the field penetration depth, and B_{eff} the effective magnetic

flux density responding to the rf field. According to Portis *et al.*,[29] the surface resistance taking vortex dissipation into account can be represented in the form

$$R_s = X_0\left[\frac{-1+(1+4B_{\rm eff}^2/B_0^2)^{1/2}}{2}\right]^{1/2}, \qquad (6)$$

where $X_0=4\pi\omega\lambda_L^2/c^2$ is the surface reactance for $B_{\rm eff}=0$, and $B_0=8\pi\omega\eta\lambda_L^2/\Phi_0$ is the characteristic value of $B_{\rm eff}$ for which the surface impedance Z_s is defined by the vortex movement. It was assumed by Portis *et al.*[29] that $B_{\rm eff}=fH$, where f is the density of free or weakly pinned fluxons ($f\sim 0.1$). However, Ji *et al.*[28] interpreted f as a part of the length of all vortices intersecting the intergranular region in the sample. They assume that there exist intergranular vortices having a number density n_J which do not pass through granules, and intragranular vortices having a number density n_g which are pinned inside granules. Besides, the main contribution to dissipation comes only from vortices intersecting weak links since the viscosity η_J of intergranular region is much higher than that of intragranular regions η_g due to a higher resistance of the intergranular regions. According to Ji *et al.*,[28] $B_{\rm eff}=(n_J+xn_g)\Phi_0$, where x is the ratio of the intergranular volume to the total volume of the sample.

The method of contactless monitoring of the HTSC response to millimeter (mm) waves was developed by our group in the beginning of 1990's (see Refs. 11 and 30). The technique is based on monitoring using rf bias whose advantages over conventional four-probe technique were known long before the discovery of HTSC.[31] Medvedev *et al.*[31] showed that the use of rf bias increases the sensitivity of detectors and improves their noise characteristics. This method makes it possible to monitor the response simultaneously in two frequency ranges, viz., rf ($\sim$10 MHz) by including a superimposed inductance coil in the resonance circuit of the quality-factor meter, and the mm range ($\sim$36 GHz) by using a quasioptical dielectric resonator which is also used for supplying a powerful mm-range signal. Details of the experimental technique are described in Refs. 30 and 32.

Investigations of the rf response of ceramic and thin-film samples of YBaCuO to mm radiation show[30,32,33] that, in the superconducting transition region, the response is complex and contains bolometric and nonbolometric components. It was found that the peak of the overall response is displaced relative to the peak of the temperature derivative dR_s/dT of the surface resistance, which describes the purely bolometric effect, by 0.4–0.7 K, depending on the quality of the sample. The displacement of peaks on the temperature scale was reduced by improving the electromagnetic characteristics of the samples (by decreasing R_s and reducing the transition width ΔT). Measurements of the relaxation response after switching off the mm wave pumping radiation[32,33] show a good agreement with various theoretical models describing the relaxation of magnetization of superconductors in the magnetic flux creep regime. The activation energy $U_0=0.05-0.5$ eV obtained from our measurements in the temperature range 77–86 K are in reasonable agreement with the experimental results presented in Refs. 28 and 34. Finally the

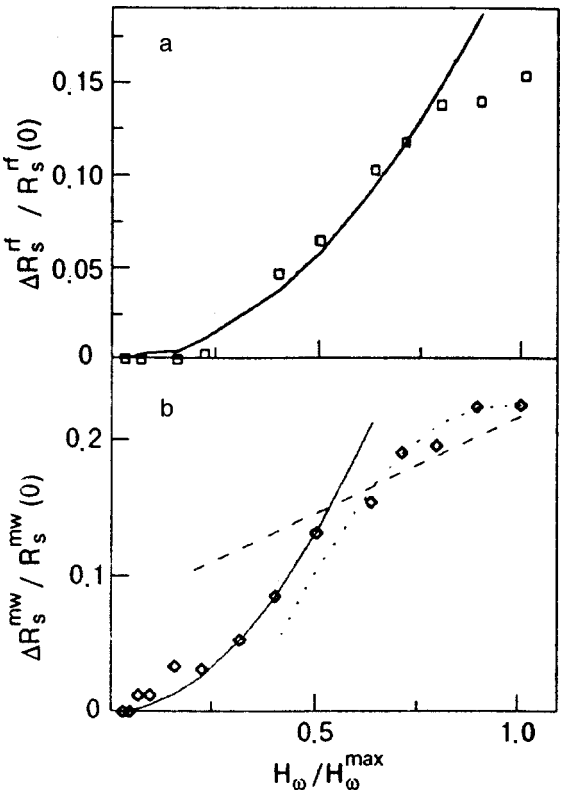

FIG. 2. Magnetic-field dependences of normalized responses of a YBaCuO thin film TF1 at $T=86.7$ K: radiofrequency response $\Delta R_s^{\rm rf}/R_s^{\rm rf}(0)$ (a) and microwave response $\Delta R_s^{\rm mw}/R_s^{\rm mw}(0)$ (b). Solid curves describe the approximation according to the Halbritter theory[35] (from Velichko *et al.*[32]).

amplitude dependences of the response of YBaCuO samples of various qualities are also described quite well by theoretical models taking into account the formation and movement of magnetic vortices under the action of a strong rf radiation.[35–37] Figures 2 and 3 show the amplitude dependences of rf and MW response of two thin films of YBaCuO deposited on a $LaAlO_3$ substrate and a YBaCuO ceramic plate, as well as the theoretical dependences obtained by using the models proposed by Halbritter,[35] Sridhar[36] and Gurevich,[37] which are in good agreement with the experimental results. Thus, it can be assumed on the basis of the results of measurements that the rf response of YBaCuO superconductors contains a nonbolometric component in the superconducting transition region. In all probability, the nonequilibrium response mechanism is associated with the creation and movement of Josephson vortices or similar magnetic vortices in inter- and intragranular weak couplings under the effect of millimeter radiation.

Salient features and conditions for realization of the mechanism

(1) The contribution to the dc resistance from the vortex movement is described by formulas (1) (in the case of creep), (4) (for flux flow), and (5) for rf R_s.
(2) The flux creep regime is characterized by an exponential temperature dependence of the resistance (see formula (1)).
(3) The flux creep regime is characterized by a linear IVC for bias currents I satisfying the condition $IHV_c r_p$

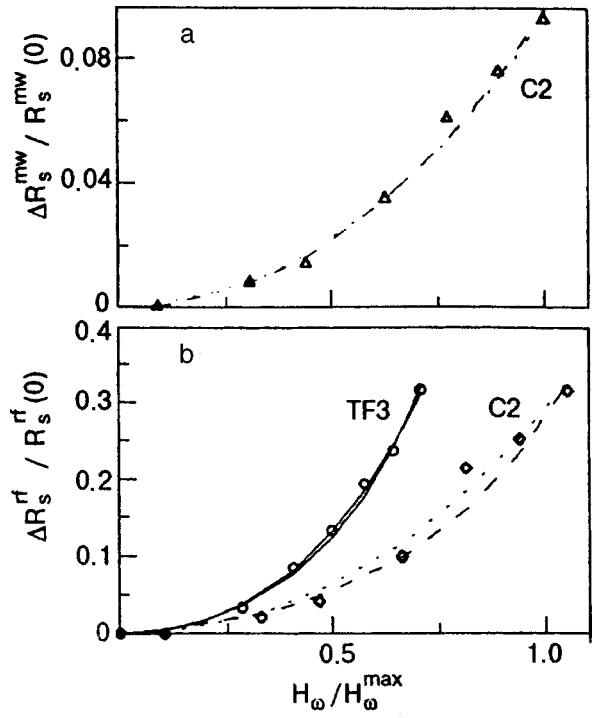

FIG. 3. Magnetic field dependence of the normalized microwave response $\Delta R_s^{mw}/R_s^{mw}(0)$ for a YBaCuO ceramic plate C2 (*a*) and radiofrequency response $\Delta R_s^{rf}/R_s^{rf}(0)$ for C2 ceramics and thin film TF3 (*b*) for 86.1 K $<T<$90.5 K. Solid and dotted curves correspond to the approximation according to Gurevich[34] and Sridhar[36] (from Velichko *et al.*[30]).

$\leqslant k_B T$ (V_c is the correlation volume and r_p is the pinning potential range), and by an exponential $V(I)$ dependence for large currents.

(4) The magnetic field dependence of resistance is described by formula (2) and is determined by the magnetic field dependence (3) of the activation energy.
(5) The response amplitude ΔR is proportional to $f_{\text{mod}}^{1/2}$, where f_{mod} is the modulation frequency of the radiation.
(6) The flux flow regime is characterized by a linear magnetic field dependence (see formula (4)) and a linear IVC ($V \approx I$).

2.2. Phase slip

A special resistive state is formed in long and narrow superconducting channels [transverse size of the channel $d_c < \xi(T)$], as well as in narrow and even wide thin films for $I > I_c$ both for $I_c = I_c^{GL}$ (I_c^{GL} is the Ginzburg–Landau depairing current) and in an external magnetic field higher than a certain value H_e' ($H_e' = \pi\Phi_0/4w^2$ is the field corresponding to penetration of metastable vortices into a film, and w is the film width). This state cannot be explained just in terms of a dynamic mixed state (DMS)[38] since for high voltages emerging under these conditions, the vortex velocity $v = V/LB$, where L is the sample length and B the magnetic induction, must be of the order of the Fermi velocity, which is evidently not feasible from a physical point of view. High condensate velocities v_s lead to depairing and the number density n_s of pairs begins to depend on v_s. The dependence of the superconducting current density $J_s(v_s)$ passes through a peak corresponding to J_c^{GL}. For $J > J_c^{GL}$, the number of superconducting electrons is not sufficient for the passage of transport current, and in contrast to the static case, the total current now contains the normal component J_n as well. The superconducting state continues to be thermodynamically more advantageous since $n_s(v_m) = (2/3)n_s(0)$ at the peak.

Webb and Warburton (see Ref. 19 in the paper by Dmitrenko[38]) detected in 1968 a regular structure of voltage steps on the IVC of tin whiskers and came to the conclusion that individual resistive centers are formed upon an increase in current. The sample resistance (slope of the IVC) increases after the emergence of each step. Later, Tinkham proposed a model of the resistive center called the phase slip center (PSC). He observed the main features of PSC, viz., the magnitude and constancy of differential resistance, as well as oscillations of J_s with Josephson frequency. The formation of the first PSC takes place in a narrow superconducting channel when the current becomes equal to the depairing current at the weakest spot in the sample. A further increase in current results in the motion of normal electrons, which leads to the emergence of an electric field accelerating the superconducting electrons to critical velocity. In this region, the order parameter ψ vanishes and the entire current is transported only by the normal component. However, the formation of Cooper pairs is advantageous as before, hence ψ emerges once again and a part of the current is transported by the condensate. For each such cycle, the phase difference for wave functions of Cooper pairs from opposite sides of the ''weak'' region will vary by 2π. Hence this site is called a phase slip center. Its characteristic size is determined by the distance over which ψ pulsates, and amounts to $\sim 2\lambda_E(T)$, where λ_E is the length of the voltage drop region.

For $|\psi| = 0$, this region lies in the normal state, and the electric field penetrates the adjacent superconducting regions to a depth $\sim \lambda_E$. Hence the formation of one PSC leads to the emergence of a resistance $2\rho\lambda_E/S$, where ρ is the resistivity of the material of the filament and S its cross-sectional area. The voltage drop across this resistance is associated only with the normal component $I_n = I - I_s$. Averaging of voltage across one PSC over time (taking into consideration the fact that the total current is constant and independent of time, while the supercurrent I_s pulsates between I_c and 0) gives

$$\overline{V} = 2\lambda_E \rho (I - \beta I_c)/S, \tag{7}$$

where $\beta \sim 0.5$. This simple formula correctly describes the experimental IVC. A further increase in current leads to the formation of new PSC's since new resistive regions come into play each time.[39]

Dmitrenko *et al.* (see Refs. 18 and 55 in their paper[38]) were the first to observe oscillations of the first derivatives of IVC of wide films in the vicinity of T_c, which were interpreted as analogs of PSC. For an applied magnetic field $H_\perp = 0$, the critical current I_c is close to the depairing current and decreases linearly with H as it increases to a certain value H' after which it oscillates with a period ΔH, while the oscillation amplitude increases with decreasing temperature. The period of these oscillations is associated with the

periodic modulation of the screening current of the potential edge barrier which hinders the vortex movement. Such a step structure of IVC of wide films was interpreted as the emergence of phase slip lines (PSL) (see Refs. 57 and 58 in the paper[38]). It was found that the IVC of a vortex-free state of a film of width $w \geqslant \lambda_\perp$ ($\lambda_\perp = 2\lambda^2/d$ is the effective field penetration depth in a film of thickness d) for $H < H'$ is similar to the IVC of a narrow superconducting channel with PSC, as in the case $H_\perp = 0$. However, the emergence and movement of vortices in a film for $H > H'$ does not change qualitatively the character of steps on the IVC. The voltage jump is preceded by a nonlinear region corresponding to DMS. Vortex movement is also a phase slip, since the passage of a single vortex through the film corresponds to a variation of the phase difference at the film edges by 2π. However, the mechanisms of PSC and PSL in wide films are quite different from the vortex mechanism.[38] It turns out that the stringent condition of a ''narrow'' ($d, w \ll \lambda_\perp$) superconducting channel is not necessary for the formation of a PSC. Moreover, the step structure of IVC of wide films is observed in zero magnetic fields also.

One of the first observations of radiation-induced phase slip in HTSC was reported by Leung *et al.*[10] who studied the optical response of granular YBaCuO films on sapphire substrates. Between T_c (temperature corresponding to zero resistance) and T_{c0} (temperature corresponding to the onset of superconducting transition), most intergranular links become nonsuperconducting, and the dc conductivity is associated with individual isolated channels in which the Josephson coupling is still strong. The size and number of such channels decreases with increasing temperature, and the response amplitude becomes smaller.[10] Obviously, the peak of the response emerges at a temperature at which most of the JJ with almost identical critical parameters (critical current, etc.) change upon exposure to radiation. The dependence of the phase slip resistance on activation energy for strongly suppressed JJ was obtained theoretically by Ambegaokar and Halperin [formula (2) in Ref. 23], and can be presented in the following form if we take into account the temperature and magnetic field dependence of U_0 from the theory developed by Yeshurun and Malozemoff (formula (3) in Ref. 24):

$$\rho_{ps}(H,T) = \rho_n \left[I_0 \left(\frac{A_T (1 - T/T_c)^{3/2}}{2H} \right) \right]^2 \tag{8}$$

where A_T is a coefficient. According to Blackstead *et al.*,[40] the passage of transport current with energy exceeding U_0 for $H > H_{c1}$ (H_{c1} is the lower critical field) causes a flux flow whose resistance is defined by formula (4). However, $\rho_{ff} = \rho_n$ in the vicinity of T_c, and hence the resistance in this region will be double the normal state resistance, which is apparently not possible physically. This can be avoided by making the substitution $\rho_n \to \rho_n - \rho(H,T)$. This gives

$$\rho_{ff} = [\rho_n - \rho(H,T)] \frac{H}{H_{c2}}. \tag{9}$$

Here, $\rho(H,T) \equiv \rho_{ps}(H,T)$ from formula (8). Taking into consideration the angle φ between the current and the magnetic field in the (**ab**) plane, we obtain[40]

$$\rho_{ff} = [\rho_n - \rho(H,T)] \frac{H}{H_{c2}} \sin^2(\varphi). \tag{10}$$

Thus, two competing mechanisms exist for $H > H_{c1}$, viz., the flux flow and the phase slip. The phase slip process is independent of the relative orientation of the current and magnetic field, and accounts for the non-Lorentzian dissipation observed in a number of works (see, for example, Ref. 41). It should be remarked that a dependence of the type (8) is manifested clearly only in the case when $H \| I$. In all other cases, the dependence $\rho(H,T)$ is determined by the flux creep regime (see Eq. (1)).

Formula (8) was obtained by Tinkham[22] for describing the dependence of the superconducting transition width on the magnetic field. However, as $H \to 0$, formula (8) gives a nonphysical value of the resistance and zero transition width. This contradiction is removed by assuming the existence of an effective intrinsic field $H_0 \neq 0$ which ensures a finite height of the energy barrier U_0 even in a zero external field. The existence of such a field is explained physically by the Kosterlitz–Thouless theory[42] which assumes the existence of thermally induced ''vortex–antivortex'' pairs below T_c. It is found that the current-induced depairing of vortex pairs leads to nonohmic losses for $H = 0$.[43] Taking such a dependence into account, we can present formula (8) in the form[43]

$$\rho_{ps}(H,T) = \rho_n \left\{ I_0 \left(\frac{A_T (1 - T/T_c)^{3/2}}{2(H + H_0)} \right) \left(1 - \frac{I}{I_{c0}} \right)^{3/2} \right\}^{-2}. \tag{11}$$

Typical values of H_0 for high-quality YBaCuO samples are $\sim 0.1 - 0.25$ T, while $H_0 \sim 0.05$ T for BiSrCaCuO.[43] For high-quality YBaCuO single crystals (see Ref. 41), the experimental data for $H = 0$ are approximated quite well for $A_T = 10.044 k_B T$. It is found that the narrower the superconducting transition, the higher the value of A_T. Moreover, the resistance calculated by using formula (11) is quite sensitive to the choice of T_{c0}, and hence a variation of T_{c0} even by 0.05 K strongly affects the value of ρ:

$$\rho = \rho_{ff} + \rho_{ps}. \tag{12}$$

It is also assumed that T_{c0} does not change in an applied magnetic field.

According to Blackstead,[43] the disordered distribution of oxygen in Cu–O planes leads to discontinuities, and a network of JJ parallel to the **c**-axis is formed between overlapping regions of adjacent planes and creates conducting channels between planes. The critical current of the entire channel is determined by the weakest junction. Thermal fluctuations lead to a relative displacement of fragments of the Cu–O planes, and perturbation of vortices pinned at these fragments leads to a time-dependent local phase difference. This results in a field dependence of resistance that is not associated with the Lorentz force.

Thus, in view of the leading role of thermal fluctuations near T_c, the dominating loss mechanism is the phase slip associated with the nanogranular nature of HTSC, i.e., with the thermal-phonon-modulated bonds between planes. According to Blackstead,[43] the resistance to flux flow dominates

at lower temperatures and hence determines the losses in granules (for YBaCuO, this temperature range corresponds to $T \leqslant 85$ K).[40]

Formula (12), in which ρ_{ff} and ρ_{ps} are defined by formulas (10) and (11) respectively, corresponds to the dc resistance. In order to determine the MW response, it is essential to know the behavior of R_s. According to Blackstead,[40] we obtain by taking residual resistance $\rho_{00} \sim 2.5 \cdot 10^{-4} \rho_n$ into consideration:

$$R_s = [(\rho_{ff} + \rho_{ps} + \rho_{00})(\omega\mu/2)]^{1/2}, \tag{13}$$

where μ is the permeability.

Dmitriev *et al.*[44] studied the effect of MW field on the behavior of PSC and observed a suppression (even disappearance) of the critical current of samples by MW radiation. They also found that in the bridges made of YBaCuO ceramics (MW radiation leads to the emergence of discrete formations that are multiples of current PSC and are called ''rf PSC'').[44] Among other things, this is confirmed by the root dependence of the response on radiation power which is characteristic of the PSC formation mechanism. It is interesting to study the dynamics of rf and current PSC observed by Dmitriev *et al.*[44] The rf PSC vanishes in a direct current, and is replaced by a current PSC. This is accompanied by a transition of the sample to the ''unperturbed'' resistive state (with zero radiation power $P_\omega = 0$).

Salient features and conditions for realization of the mechanism

(1) The IVC of superconducting channels in which PSC are formed is described by Eq. (7).
(2) The dependence of phase slip resistance on temperature, magnetic field and bias current is described by formula (11). This mechanism is especially clearly manifested for parallel orientation of current and magnetic field along the **c**-axis since there is no contribution from the flux flow in this case. In view of the thermal activation nature of the process, it is manifested quite strongly in the vicinity of T_c.
(3) The phase slip resistance is independent of the angle between the current and the magnetic field.
(4) The response amplitude increases in proportion to the square root of the radiation power.

2.3. Breaking of ''vortex–antivotex'' pairs

A large number of publications (see, for example, Ref. 45) report on the nonbolometric detection of infrared (IR) radiation in thin HTSC films. This regime is characterized by an anomalously large responsivity R_v approaching the quantum limit $R_v = 1/(2e\nu)$. In order to explain this effect, Kadin *et al.*[46] proposed a model for photon-induced dissociation of vortex pairs existing in two-dimensional superconductors. The theory of vortices in two-dimensional superconductors[42] assumes the presence of ''vortex–antivortex'' (V-AV) pairs below T_c which effectively screen vortex interaction at high temperatures and lead to the formation of free vortices. Under the action of transport current, these vortices move and lead to energy dissipation. As the temperature is lowered, most of the vortex pairs ''freeze out'' and a second phase transition, called Kosterlitz–Thouless transition, occurs at a temperature T_{KT} and is accompanied by a pairing of all free vortices. Below T_{KT}, all vortices are paired, and there is no dissipation associated with their movement.[46] The formation of vortex pairs takes place through the emergence of a vortex ''core'' on the scale of the coherence length ξ with a local suppression of the order parameter ($\Delta = 0$). This may be caused by thermal fluctuations or by the photons of the incident radiation.[47] If vortices are separated in space, i.e., do not overlap, the currents circulating around the core become significant and the vortices are stable. The energy of such a pair, separated by a distance $r \gg \xi$, can be represented in the form[47]

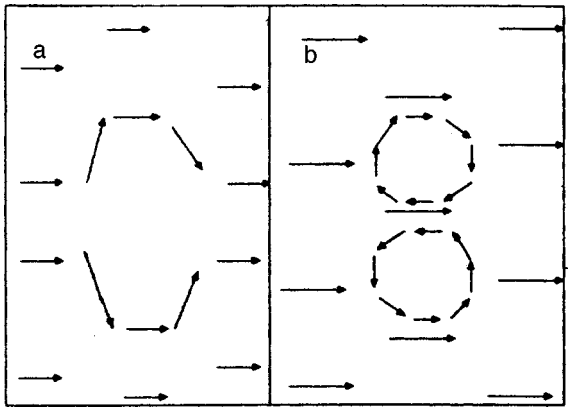

FIG. 4. The pattern of current flow near a ''vortex–antivortex'' pair generated for a large transport current: total current (a) and the same configuration with separated vortex currents (b) (from Kadin *et al.*[46]).

$$E_v = E_{v0} \ln(r/\xi) = \Phi_0^2 d/2\pi\lambda_L^2 \ln(r/\xi). \tag{14}$$

For two closely-spaced vortices, the minimum energy E_{v0} of the vortex pair is of the order of energy of condensation in two vortex cores. As a rule, this energy is much higher than Δ. The above equation also gives the energy of attraction between vortices which is overcome by the Lorentz force emerging as a result of the passage of a current with density $J = E_{v0}/\Phi_0 r d$. For $r = \xi$, the current density J approaches the critical value J_c, thus indicating that a vortex pair may be formed by current alone. Such a model is a two-dimensional generalization of the model of PSC formation in a superconducting microstrip.[48] Figure 4 shows the current configuration in the vicinity of a vortex-pair being formed. For $T < T_{\mathrm{KT}} = E_{v0}/4k_B$, the breaking of the vortex pair may be caused by the current, resulting in a nonlinear IVC of the type $V \approx I^n$. Depending on temperature, three regimes with different IVC can be singled out:

$$V(I) = \begin{cases} \sim (I - I_c)^n, \quad n > 3 & \text{for } T \ll T_{KT}, \quad I > I_c, \\ \sim I^3 & \text{for } T = T_{KT}, \\ \sim I \text{ for } T > T_{KT} & \text{for small } I. \end{cases} \tag{15}$$

Such a form of IVC is caused by thermal activation processes leading to a nonlinear resistance of the form

$$R(J) \sim \exp\left(-\frac{E_v(J)}{2k_B T}\right) \simeq (J/J_c)^{E_{v0}/2k_B T}. \tag{16}$$

This equation is valid for $J \leqslant J_c$. For very small bias currents, the resistance is defined by the expression

$$R/R_{\max} = a \exp[-2(b/\tau)^{1/2}], \tag{17}$$

where $\tau = (T - T_{\mathrm{KT}})/(T_{c0} - T)$, a and b are constants, and $R_{\max}$ is the resistance at temperatures above T_{c0}.

Kadin *et al.*[46] propose the following microscopic mechanism of formation of V-AV pairs as a result of photon absorption. A photon with energy $h\nu \gg 2\Delta$ is absorbed in a certain region (spot) at the surface of a $2D$ film, giving rise to a pair of highly excited quasiparticles which break additional Cooper pairs over a time period of the order of a few microseconds and distribute the excess energy among a large number of quasiparticles. These quasiparticles diffuse into the film over a depth $\sim\xi$ over a time $\sim h/k_B T_{KT}$ and suppress the order parameter Δ in this layer, as well as the critical current I_c. If the value of I_c in the region of the spot is smaller than the transport current I, this will lead to instability and a local collapse of Δ, causing the screening current to bend around this ''hot spot.'' This process is analogous to phase slip induced by the phonon absorption, which provides the additional energy required by the current for the formation of a vortex pair (see Fig. 4). As a result of further diffusion of nonequilibrium quasiparticles into the film, the hot spot vanishes. However, the vortices continue to move at right angles to the current until they reach the edge of the film, leading to the emergence of a magnetic flux Φ_0 through the film which is equivalent to an integral voltage pulse. The time-averaged responsivity is given by $R_v = 1/(2e\nu)$.

The model described above, which was proposed for a homogeneous (on the scale $\sim\xi$) two-dimensional superconductor, can also be used for describing a $2D$ chain of weakly coupled JJ. It should be recalled that the effective field penetration depth λ_{eff} corresponding to weak intergranular currents may be quite large. Intergranular vortices with a reduced nucleation energy, and hence with a reduced pair dissociation energy, may emerge in such films. This explains the observed transition to vortex depairing in ordered chains of junctions as well as in granular superconductors. As soon as a vortex pair is formed, it behaves essentially in the same way as in a homogeneous film. For a granular superconductor with granule size $\leqslant\xi$, a photon absorbed in one of the granules suppresses Δ over the entire film, and reduces the critical currents linking it with the adjoining granules. This causes a local deviation of the current (Fig. 4a) followed by the formation of a vortex pair (Fig. 4b). In superconductors with a large size of the granules, however, a photon absorbed at the center of a granule hardly affects the intergranular currents. If the coupling between granules is not quite uniform, the vortex pairs formed in such granules cannot be dissociated by the current passing through them. In both these cases, the quantum efficiency of the process will be considerably reduced, which explains the large spread in the experimentally observed values of responsivity for granular thin-film HTSC detectors.

In spite of the fact that the formation of vortex pairs in this model occurs due to local heating, it was observed[49] that this is a nonequilibrium process and hence does not suffer from the drawbacks of bolometric detection. In this case, the total heating of the film is quite insignificant while the local heating may be quite strong. Kadin *et al.*[49] proposed two possible regimes of formation of vortex pairs. For $h\nu < \Delta$, the absorption of a quantum is linked directly with the formation of a vortex pair. Such a pair is formed in two cases: (1) if the energy of the quantum at a given temperature is higher than the nucleation energy E_{v0}, and (2) if the total current $I_\Sigma = I + I_\omega$ (I is the bias current and I_ω the ac amplitude) exceeds the critical current I_c over a time long enough for the formation of a vortex. For $h\nu > \Delta$, Cooper pairs are dissociated at first. This is followed by the formation of a vortex pair as a result of local heating.

The response time in this model is determined by the fluxon velocity $v = J\Phi_0/\eta = J\rho_n 2\pi\xi^2/\Phi_0$ in a direction perpendicular to the applied current, where η is the viscosity of vortices in the Bardeen–Stefan theory, and ρ_n is the resistivity in the normal state. For $J \sim J_c$, since $J_c\rho_n \simeq \Delta/e\xi$, we obtain the velocity $v \simeq \Delta\xi/h$ which approaches the Fermi velocity $v_F = 10^7 - 10^8$ cm/s for a pure superconductor. For a film of width $w = 10\ \mu$m and $v_F = 10^7$ cm/s, we obtain the response time $t_R = 100$ ps. For sensitivity optimization, the working temperature must be lower than T_{KT} since the sensitivity at higher temperatures will be limited by the background voltage associated with thermally activated unpaired vortices and the magnetic field induced by the current.[49] The most suitable material for a detector is a film with uniformly linked small granules, for which the injection of vortices from the film edges is restricted. The absorption of a photon in HTSC leads to the formation of a vortex ring (three-dimensional analog of a $2D$ vortex pair) which is enlarged by the transport current and splits into a V–AV pair upon reaching the (lower and upper) film surface, leading to the same responsivity $R_v = \Phi_0/h\nu$. In the one-dimensional case of a long wire with cross-sectional size $\sim\xi$, the absorption of a photon leads to the formation of a PSC which produces voltage steps.[46] For the one-dimensional case, the photon absorption may be accompanied by the formation of more than one PSC, which leads to an enhanced sensitivity below the quantum limit. In all other cases, the sensitivity of a film displaced in the vicinity of J_c is confined by the quantum limit since the violation of superconductivity due to the absorption of a photon is always connected with some kind of phase slip or a vortex process for which the magnetic flux quantum is a characteristic quantity.

Johnson *et al.*[50] studied the response of 10 nm-thick granular NbN films (with a grain size of the order of the film thickness) on Si substrates to optical radiation of wavelength $\Lambda = 632$ and 670 nm with a modulation frequency < 3.7 kHz and > 100 kHz, respectively. Meander-shaped structures with a constant surface area of 10^{-4} cm^2 ($5 \times 200\mu$m, $10 \times 100\mu$m, etc.) were prepared from these films. Below T_c, the authors[50] observed a slow bolometric response associated with film heating together with the substrate. It was found that radiation with wavelength $\leqslant 1\ \mu$m is absorbed strongly by Si and produces charge carriers in it. If the NbN film is displaced towards higher differential resistance, the conducting Si substrate partially shunts the response of the superconductor. In this case, the response becomes negative, i.e., the response amplitude decreases with increasing radiation

power. While the total response to continuous irradiation is positive, an increase in the modulation frequency transforms a slow positive signal into a fast negative signal. For high modulation frequencies, the slow bolometric response cannot ''catch up'' with the negative shunting component, and the net response is negative. In the absence of a bias current, when the laser beam is centered in the meander region, a rapid response which does not depend on the modulation frequency f_{mod} was observed up to 100 kHz. The authors associate this response with the photoelectric effect at the interface between NbN and Si. The photoelectric effect was not observed during optimization of the rapid positive component through an appropriate choice of the position of the laser beam.

The authors studied the transient and steady-state response as a function of the bias current I_b and temperature for $I_b<I_c$ and $T<T_c$. It was found that the dependences of the response δV_{ac} on $(\delta V/\delta T)_I$ are considerably nonlinear, especially in a constant weak magnetic field (up to 100 Oe). The nonlinear part of the dependence was observed for I_b corresponding to the highest differential resistance, and hence the shunting effect of the substrate was very strong. Measurement of $(\delta V/\delta T)_{I_b}$ for small I_b were used by the authors to estimate the effective sample heating δT_{eff} $\sim$150 mK. The highest responsivity R_v was observed in currents close to I_b and was 125 V/W. Under the assumption that the positive response is associated only with the bolometric effect, the effective heating is theoretically estimated at 1–11 mK, which is much smaller than the experimental value. It is assumed that the observed response may be caused by two nonequilibrium mechanisms, i.e., either by electron heating effect, or by the kinetic inductivity mechanism. The former gives an extremely low value of δT_{eff} $\sim$1 mK, as well as an underestimated value of responsivity. The authors believe that the photofluxon model of vortex-pair formation may explain the observed response, although the value of responsivity $R_v \sim 10^4$ V/W predicted by this model is much higher than the experimental value of 125 V/W. To prevent the excitation of photocarriers in Si and to avoid shunting of the response by the substrate, the same authors used a longer wavelength radiation source, viz., a diode laser with $\Lambda = 1300$ nm, in their later work[9] for a clearer differentiation of the response mechanisms. In the absence of a bias current, the responsivity of the response at radiation wavelengths 670 and 1300 nm was $\sim$20 V/W. When the laser beam was centered on the meander, a positive response was observed. This response persisted as the frequency f_{mod} was increased to 1 MHz, and was attributed by the authors to the heating of the NbN film relative to the substrate. The response amplitude varied linearly with the radiation intensity, and the modulated response signal remained purely sinusoidal without any harmonics. The responsivity for rapid response was estimated at $\sim$1500 V/W. The maximum possible heating of the sample did not exceed 2 mK.

Measurements of the dependence of the response on bias current and IVC at various temperatures led to the resistance $R_{\mathrm{eff}}^{(T)}$ of the thermal boundary between the film and the substrate. It was found that $R_{\mathrm{eff}}^{(T)}$ depends strongly on I_b, while for a purely thermal effect it should not depend on current, but must have a significant temperature dependence. A comparison of the experimental results with the hot spot model[51] reveals a good agreement for the temperature dependence of $R_{\mathrm{eff}}^{(T)}$ near the transition, while the value of $R_{\mathrm{eff}}^{(T)}$ obtained from the model for a deep superconducting state is found to be too low. It is borne out by computations[9] that the thermal resistance $R_{e\mathrm{ph}}^{(T)}$ associated with a finite time $\tau_{e\mathrm{ph}}$ of energy transfer from electrons to phonons in the film makes a decisive contribution to the time characteristics of the response as compared with the Kapitza thermal resistance R_{K} due to a finite time of energy transfer from the phonons in the film to the phonons in the substrate.

Since the thermal conductivity estimates used in the model include the electron heating effect, and the quantity $(\partial V/\partial T)_{I_b}$ (which is also used in the model) takes into account the thermal effects associated with the weak links between granules, the authors do not believe that these effects can explain the observed response. The response amplitude estimated from the kinetic inductivity variation mechanism is also too low (0.04 μW obtained from theory against an experimental value 100 μW). However, the experimentally observed response time of about 1 ns is of the same order as the value estimated by using the photofluxon model. For an unambiguous conclusion concerning the applicability of the photofluxon model, we must carry out experiments with a subnanosecond resolution and measure the dependence of the response time on the film thickness, which must be linear.[9]

Salient features and conditions for realization of the mechanism

(1) The dependence of the resistance associated with the dissociation of the V–AV pairs on temperature and bias current I is obtained by using formulas (16) and (17).
(2) Formula (15) describes the IVC at different temperatures and for different bias currents.
(3) The limiting sensitivity of this mechanism is equal to $\Phi_0/h\nu$.
(4) The response time for $v_F = 10^7$ cm/s and a film width $w = 10$ μm is $\sim$100 ps.
(5) The sensitivity can be increased right up to the quantum limit by decreasing the working temperature to below T_{KT} and selecting a film made of uniformly linked small size granules.

2.4. Inverse AC Josephson effect

The emergence of a dc voltage across JJ formed by a low-temperature superconductor under the action of microwave radiation was observed for the first time by Langerberg *et al.*[52] This phenomenon known as the inverse ac Josephson effect served as an impetus in the study of possible applications of JJ as EMR detectors. The discovery of HTSC stimulated a number of publications[53–56] in which the observed nonbolometric response of HTSC was interpreted as a modulation of weak-link parameters (critical current, order parameter phase, etc.) by an induced rf current.

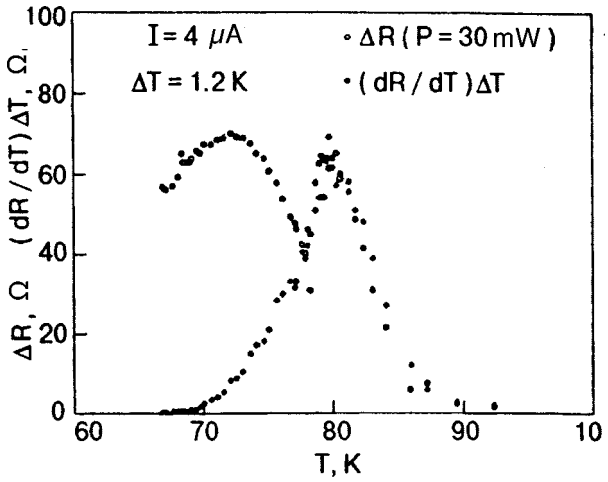

FIG. 5. Temperature dependences of the response ΔR and derivative dR/dT multiplied by the constant $\Delta T = 1.2$ K for a YBaCuO film (from Chang *et al.*[54]).

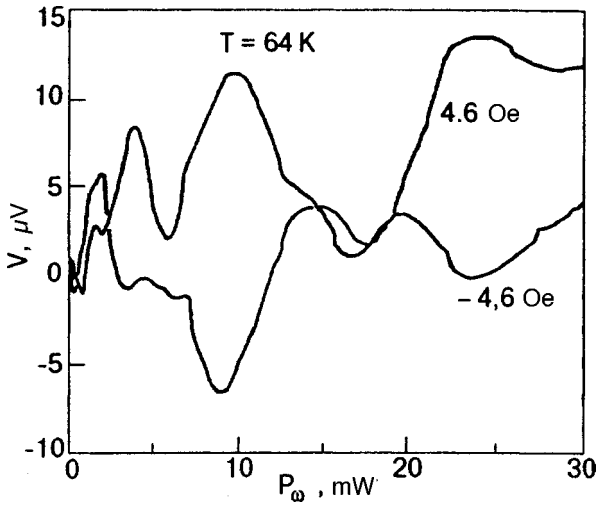

FIG. 6. Dependence of the voltage V induced by microwave radiation on the microwave power of a YBaCuO film in the absence of a constant bias for two different directions of the constant magnetic field at $T = 64$ K (from Chang *et al.*[54]).

Durny *et al.*[53] studied YBaCuO ceramic samples in the form of rectangular bars placed in the cavity of EPR spectrometer. The voltage induced in the sample by MW radiation (9.42 GHz) was measured as a function of temperature T, constant field H, and radiation power P_ω. It was found that the magnetic field suppresses the response for any field polarity. The amplitude ΔV of the response increased with decreasing T and increasing P_ω. The $\Delta V(P_\omega)$ dependence was linear in the P_ω range from 1 to 100 mW at low ($\sim$31 K) and high ($\sim$81 K) temperatures. In the intermediate temperature range (50–70 K), weak saturation of the $\Delta V(P_\omega)$ dependence was observed for $P_\omega \sim 20-30$ mW. Durny at al.[53] associate the response mechanism with the motion of Josephson vortices formed in weak links under the action of the Lorentz force exerted by the transport current.

Chang *et al.*[54] studied granular YBaCuO films in the form of an ''H''-structure. An ''H''-shaped film was placed in a rectangular waveguide so that the electric field $\mathbf{E}_\omega$ was parallel to the ''bridge,'' while the magnetic field $\mathbf{H}_\omega$ was perpendicular to the plane of the H-structure. Such an experimental geometry makes it possible to create an optimal coupling with $\mathbf{H}_\omega$ and prevents the interaction with the electric component, which permits to avoid ordinary rectification effects which are not associated with the physics of HTSC. A quasi-homogeneous chain of JJ is formed in the bridge of the H-structure, for which the dependence of ΔV on H (or H_ω) is strictly periodic in contrast to a randomly oriented $3D$ chain, since weak links respond to radiation synchronously. Chang *et al.*[54] discovered that the temperature dependence of the response $\Delta R = R(P_\omega) - R(0)$ exhibits two peaks (Fig. 5). The high-temperature peak is correctly described by the dependence

$$\Delta R = (dR/dT)\Delta T, \tag{18}$$

typical of the bolometric mechanism. The low-temperature peak of the response is in the tail of the resistive transition, where $dR/dT \to 0$ and is obviously not of thermal origin. The dependence on microwave power ($P_\omega^{\max} \sim 30$ mW) is linear in the region of the high-temperature peak, which confirms the bolometric nature of the response, while $\Delta R \propto \log(P_\omega)$ in the temperature range in which a nonbolometric response is observed. According to Chang *et al.*,[54] the time variation of the order parameter phase φ induced in a long JJ by MW radiation (even in zero magnetic field) leads to the formation of vortices which can move under the action of a direct transport current. The response amplitude ΔV in this case is proportional to the number of JJ that respond synchronously to radiation for a given I_b. It was found that the nonbolometric peak of the response increases and is displaced towards low temperatures upon an increase in the bias current as well as in the MW power. The response appears under the condition $I_b > I_c$. Chang *et al.*[54] state that the mechanism of induced motion of vortices proposed by them causes a response similar to that observed during dissociation of V–AV pairs in the course of a Kosterlitz–Thouless transition.[45] However, the IVC is linear ($V \approx I$) for this mechanism in the vicinity of T_c, while $V \approx I^3$ in the case of dissociation of vortex pairs. In addition, the oscillating dependence of ΔV on P_ω for $H = \text{const}$ (Fig. 6) and on H for $P_\omega = \text{const}$ unambiguously suggest the Josephson mechanism of the response, in which the vortices generated by a weak magnetic field move under the action of the current induced by MW radiation, leading to voltage oscillations.

Gallop *et al.*[55] observed the dependence of the differential resistance dV/dI of YBaCuO and BiSrCaCuO films on a MgO substrate on the bias voltage V_b under the effect of MW radiation ($\sim$10 mW) of frequency 8–20 GHz. The difference in the differential resistance in the presence of radiation and without it is of a periodic oscillating form with peaks at $V_b = n\Phi_0\nu$, where n is an integer and ν the radiation frequency. We assume that the fluxon lattice observed in YBaCuO at low temperatures moves under the action of the rf current, which induces the voltage $V = d\Phi/dT = mv(I_b\Phi_0)$ according to Faraday's law (m is the number of fluxons per unit area and $v(I_b)$ the velocity of fluxons, which strongly depends on the bias current I_b). The motion of flow

in this case is synchronized with the applied MW voltage within a limited range of V_b so that the velocity of fluxon motion through a superconducting microstrip is $dN/dt = n\nu$. In this case, the voltage drop across the film in this synchronized state is $V=\Phi_0(dN/dt)=n\Phi_0\nu$. This condition is similar to the condition for the formation of a Shapiro step in a solitary JJ.

Boone *et al.*[56] also studied the response of YBaCuO films in the form of 2000×600 μm strips of thickness 1.3–2 μm to pulsed MW radiation of frequency 9 GHz. The response observed in the region of resistive ''tail'' increases with I_b and with MW power ($P_\omega^{\max}\sim 100$ mW). It was found that the response amplitude is independent of the modulation frequency, which is typical of a nonbolometric response. The noise voltage measured with the help of a synchronous detector (in the absence of radiation), as well as the response itself, had a peak in the region of the resistive tail. The noise measurements permitted the estimation of the noise equivalent power (NEP) $P_{\text{eq}}\sim 6\cdot 10^{-10}$ W/$\sqrt{\text{Hz}}$, the responsivity being 136 V/W. Among possible mechanisms of response, the radiation-induced flux flow within intergranular weak links is considered. The mechanisms of dissociation of V–AV pairs,[45] photoinduced flux creep,[17] and synchronization of the fluxon lattice with the MW field[55] are not ruled out either.

Huggard *et al.*[57] studied the response of BiSrCaCuO thin-film bridges to the pulsed ($\tau=65$ ns) IR radiation ($\Lambda = 447$ μm) with the pulse repetition frequency of 165 Hz. The observed broadening of the decreasing component to the output pulse as compared to the input pulse can be explained by the nonlinearity of the response. As the current I_b increases, the peak of the response corresponding to the end of the resistive tail was shifted towards low temperatures right up to complete vanishing of the response for $I_b>100$ μA. The amplitude of the response was proportional to $\sqrt{P_\omega}$ in the case of high radiation powers and was linear in P_ω for low powers. The two methods of estimating NEP and responsivity mentioned above lead to the following results: $P_{\text{eq}}=5\cdot 10^{-9}$ W/Hz$^{1/2}$, $R_v=0.6$ V/W($1\text{ mW}<P_\omega<50$ mW) and $P_{\text{eq}}=3\cdot 10^{-12}$ W/Hz$^{1/2}$, $R_v=1.2\cdot 10^{-2}$ V/W($0<P_\omega<1$ mW). All the estimates were obtained in a detection band of 50 MHz. Huggard *et al.*[57] ruled out the bolometric origin of the response since, according to Barone and Patterno,[59] the critical current is independent of temperature at $T<T_c/3$, while the response in Ref. 57 was observed at $T=17\text{ K}\ll T_c/3$ ($T_c\sim 85$ K).

Computer simulation proved[58] that for frequencies $h\nu \ll 2\Delta$ and $I_\omega/I_0<1$, the maximum nondissipative current $I_c=I_0(1-\gamma I_\omega)$, where γ is a constant, I_ω the amplitude of the current induced by radiation, and I_0 the characteristic spread in the critical currents of JJ forming a bridge. At a working point with the differential resistance $\delta V/\delta I=R$, the voltage across the junction satisfies the equation

$$V=\gamma I_0 R I_\omega, \tag{19}$$

or $V\sim\sqrt{P_\omega}$. For $I_\omega\ll I_0$, a linear dependence on P_ω is expected.[59] Thus, Huggard *et al.*[57] proved that the response of a bridge to IR radiation is correctly described by the model of a solitary JJ in which I_c is replaced by a certain effective value I_0. This confirms the hypothesis on synchronous response of weak links to EMR.[60]

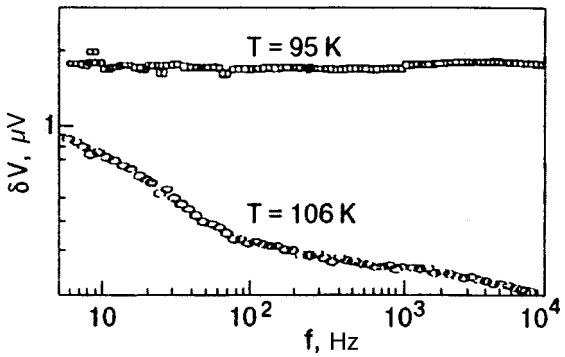

FIG. 7. Photoresponse of a BiSrCaCuO thin film as a function of the modulation frequency for the bolometric ($T=106$ K) and nonbolometric ($T=95$ K) components, $I=1$ mA and $P=2.5$ mW/cm^2 (from Ngo Phong and T. Shih[62]).

Schneider *et al.*[61] studied the frequency dependence of the response of BiSrCaCuO microbridges in the frequency range (10–1000) cm^{-1}. For frequencies varying from 10 to 100 cm^{-1}, only a nonbolometric response with a time constant $\tau\sim 4$ ns was detected with the dependence $\Delta V\sim P_\omega^{1/2}$ in the range from 3 to 30 mW. At a frequency 939 cm^{-1}, a bolometric response is also observed in addition to the nonthermal component near T_c. For $P_\omega<1$ mW, both components are linear functions of power. In this case, the response amplitude $\Delta V\sim\sqrt{P_\omega}$ for $\omega<100$ cm^{-1}, while this quantity is proportional to P_ω for $\omega=939$ cm^{-1}. The frequency dependence of the response in the frequency range from 10 to 1000 cm^{-1} is correctly described by a power law with the exponent 2.3. The obtained results confirm the Josephson nature of the nonbolometric response and rule out nonequilibrium mechanisms associated with electron heating and hot spots exhibiting a linear power dependence and *a weak frequency dependence*.

Ngo Phong and T. Shih[62] measured the response of strip structures of BiSrCaCuO granular films to 5-mm radiation. The response had high-temperature bolometric and low-temperature nonthermal components. The heating near T_c was estimated at ~ 0.3 mK. With increasing bias current, the dynamics typical of both components was observed: the high-temperature component of the response increased linearly and remained at the same temperature, while the low-temperature component increased nonlinearly, attaining saturation for large values of I_b, and was shifted towards lower temperatures. The high-temperature component as a function of modulation frequency decreased abruptly in the range $0<f_{\text{mod}}<100$ Hz and then diminished more smoothly up to 10 kHz. At the same time, the low-temperature component was virtually independent of f_{mod} (Fig. 7). The transformation of the MW pulse ($\tau\sim 50$ ms) after the interaction with the sample was also studied at three temperatures (Fig. 8). In the region of low-temperature component, the shape of the output pulse was exactly the same as that of the input pulse, demonstrating a short response time (the leading front <250 ns). The high-temperature component was character-

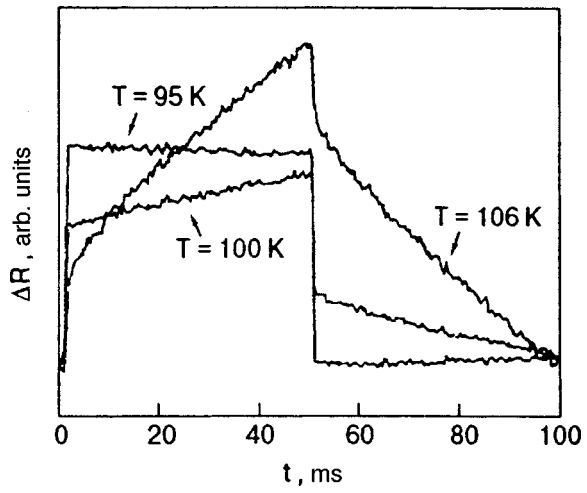

FIG. 8. Transient response ΔR of a thin YBaCuO film induced by MW ($\Lambda = 5$ mm) pulsed radiation at various temperatures near T_c, $I = 1$ mA, $f_{\text{mod}} = 10$ Hz, and $P = 2.5$ mW/cm^2 (from Ngo Phong and T. Shih[62]).

ized by a ''smeared'' asymmetric output pulse (the rise and fall times ~ 1 ms and ~ 20 ms respectively). For the intermediate temperature, the steepness of the leading front of the output pulse varied with time, indicating the presence of a thermal as well as a nonthermal component in the response. The amplitude of the nonthermal component decreased with the extent of granular structure in the sample, and the nonbolometric response was not observed at all for samples with $J_c \sim 10^5$ A/cm^2 at 77 K. The estimates of responsivity and detectability D^* under nonbolometric conditions give the values of $R_v = 10$ V/W and $D^* = 1.1 \cdot 10^8$ cm$\cdot$Hz$^{1/2}$/W. For both components, the power dependence was linear. A dependence of the form $\Delta V \sim P_\omega^{1/2}$ typical of JJ for large values of power[59] was not observed since large power levels were inaccessible. Finally, an analysis of the temperature dependence of the optical ($\Lambda \sim 1.06\ \mu$m and $\Lambda \sim 1.56\ \mu$m) and MW ($\Lambda \sim 5$ mm) responses in the same sample showed that only the bolometric component is left for $h\nu > 2\Delta$. It was emphasized that the Josephson detection mode is typical only for $h\nu < 2\Delta$.

Schneider *et al.*[3] studied recently the response of microstrips made of BiSrCaCuO films on MgO substrates to pulsed ($\sim 80\ \mu$s) IR radiation ($\Lambda \simeq 0.5$ mm) in a constant magnetic field up to 8 T. The magnetic field dependence of the response is determined by the dependence of critical current on B for a solitary rectangular JJ of thickness $d \ll \lambda_L$ and length l in a transverse magnetic field:

$$I_c(B) = I_c(0)\left|\frac{\sin[\pi(\Phi/\Phi_0)]}{\pi(\Phi/\Phi_0)}\right|. \tag{20}$$

The interference pattern is blurred in view of the spread in the parameters of weak links. Schneider *et al.*[3] proved that, according to (20), the magnetic field can either suppress ($I_b > I_c$) or enhance ($I_b < I_c$) the response depending on the relation between I_b and I_c for I_b varying from 2 to 100 μA in the magnetic field range 1 mT$< B <$ 50 mT. Since $I_c(B)$ depends on the length of the junction, Schneider *et al.* could estimate the characteristic size of junctions ($l_J \simeq 0.5\ \mu$m). For $B < 50$ mT, the $\Delta V(B)$ dependence has a plateau which is attributed by the authors to the presence of weak links of the nanometric scale with considerably higher values of I_c, which are ''immersed'' in grain boundaries. The characteristic size of such ''strong'' weak links, which was estimated from the period of the diffraction pattern, is $l_a \leqslant 1$ nm. The dependence of the response on H also exhibits a hysteresis (memory effects), and the response remains suppressed for $I_c > 20\ \mu A$ even after the removal of the field. This can be due to flux trapping in the network of granules and to the presence of weak links with high values of I_c, which form a barrier preventing the escape of vortices. However, Schneider *et al.*[3] rule out the trapping in granules themselves since it would decrease the intergranular field and lead to stimulation rather than suppression of the response.

Irie and Oya[63] studied in 1995 the response of BSCCO single crystals having a size of 1×1 to 3×5 mm and thickness 0.1–0.2 mm to MW radiation (of frequency 8–10 GHz). The measurements of the response by the four-probe technique along the **c**-axis revealed that the IVC of an exposed sample contains multiple resistive branches which are attributed by the authors to interplanar chains of series-connected JJ of the SIS type in the single crystal. For $I_b > I_c^{\min}$, a voltage is induced across the weakest junction, and a further increase in I_b leads to the formation of N jumps on IVC, corresponding to transition to the resistive state in N Josephson junctions. For low radiation power levels, the steps on IVC satisfy the relation $V_n = mn\nu/2e$, where m is the number of synchronized junctions, n is an integer (number of steps), and the shape of the IVC is similar to that for a solitary JJ. In the case of high-intensity radiation, when the signal frequency coincides with one of bulk modes of the resonator, the IVC changes significantly. It acquires steps corresponding to synchronization of fluxons with MW radiation. Finally, for large values of power, when the MW frequency does not coincide with resonator modes, vortices are not synchronized with external radiation. In this case, the flux flow mode can dominate over Josephson properties of the junction, which is also confirmed by the power dependence of the height of voltage steps, having the form $V_n \sim P_\omega^{1/2}$. In this case, neither the voltage V_p corresponding to the formation of steps, nor the amplitude I_p of a step depend on frequency in the range 8–10 GHz. In this case, the steps are considerably blurred (broadened) since the motion of fluxons is not associated with resonant modes, and irradiation plays the role of a trigger that controls the arrival of vortices in the junction.

Ling *et al.*[64] used the four-probe technique to study the response of YBaCuO single crystals to MW radiation (8–12 GHz) with or without direct measuring current along the **c**-axis. The sample was mounted at the end of the waveguide so that the MW fields H_ω and E_ω were parallel to the (ab) plane and the **c**-axis, respectively. The sliding short located at the end of the waveguide made it possible to control the position of the peaks of the electric and magnetic fields relative to the sample.

The dependence of response on the bias current in the normal state ($T = 94$ K) for various radiation powers (from 1 to 7 mW) was linear with a negative slope due to the fact that

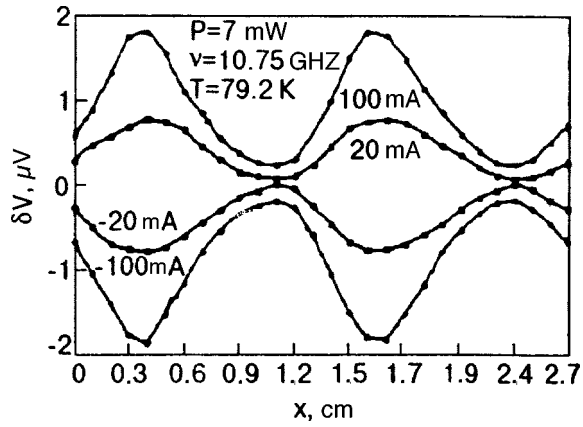

FIG. 9. Constant voltage δV induced by microwave radiation as a function of the sample coordinate for a strong current (from Ling *et al.*[64]).

the resistance along the **c**-axis in the normal state varies in proportion to $1/T$. In the superconducting state, the dependence of response on I_b has the shape of a curve with a peak displaced towards smaller currents upon an increase in the power P_ω. The response has positive polarity and an amplitude two orders of magnitude larger than in the normal state. At the same time, the current corresponding to the maximum response is equal to the critical current. The dependence of the response along the **c**-axis on the position x of the sample exhibits bipolar oscillating behavior with a period equal to 1/2 wavelength in the waveguide. The frequency dependence of the response in the range 8–12 GHz is also oscillating. This rules out rectification and differential heating associated with sample inhomogeneity as possible reasons of the response. On the other hand, such a behavior is in accord with ordinary time-dependent Josephson effect in which induced voltage varies as a Bessel's function. For $I_b=0$, no correlation between the ΔV peaks and the components E_ω and H_ω of the MW field was observed, while an increase in I_b led to clearly manifested displacement of oscillatory peaks towards maxima of the magnetic field H_ω. The height of the peaks increased with the bias current, and for large values of I_b (>20 mA) the polarity of the peaks was strictly determined by the polarity of bias current (Fig. 9). Ling *et al.*[64] attribute the observed response to the presence of intrinsic Josephson junctions in YBaCuO in the direction of the **c**-axis, in which the NW radiation induces pairs of Josephson vortices and antivortices. If $I_b\neq 0$, the formed pair of vortices is carried by current in various directions, leading to the emergence in the sample of a voltage with polarity coinciding with the polarity of I_b. For $I_b\neq 0$, the peaks of the response must coincide with the peaks of H_ω, and the polarity must be the same as that of I_b.

For $I_b=0$, vortices move under the action of MW electric field E_ω with a phase shift θ relative to H_ω in view of different phase relations for H_ω and E_ω in the Josephson junction. The resultant pattern of $\Delta V(x)$ depends on θ and has peaks separated by $\Lambda/2$. The polarity changes with the position x of the sample and can be purely positive or negative for $\theta=\pm\pi/2$.

Main features and conditions for realization of the mechanism

(1) The presence of a peak on the temperature dependence of response at temperatures much lower than the peak of the bolometric response.
(2) Displacement of the peak of the nonbolometric response towards low temperatures and a nonlinear increase (with saturation) of its amplitude with the bias current.
(3) Linear IVC of an HTSC bridge in the region of temperature corresponding to the maximum response.
(4) Independence of response of modulation frequency.
(5) Increase in the response amplitude with the extent of granular structure in the sample.
(6) Decrease in the response amplitude with the radiation frequency approximately in proportion to $\omega^{2.3}$.
(7) Linear and root dependence on radiation power for large and small power levels respectively.
(8) Stimulation of the response by a weak magnetic field for $I_b<I_c$ and its suppression for $I_b>I_c$.

2.5. Nonequilibrium breaking of cooper pairs

The properties of a superconductor below T_c are very sensitive to external excitations such as electrons, phonons, and photons.[65] In the case of MW frequencies for which $h\nu<2\Delta$. Cooper pairs cannot be broken, and the absorption of a photon is reduced to the energy redistribution of quasiparticles, which can stimulate superconductivity under certain conditions due to an increase in the gap width.[66,67] Cooper pairs can break under the interaction of the superconductor with EMR whose energy quantum $h\nu>2\Delta$ (light and IR radiation). Optical photons have energy of the order of several eV, while the energy corresponding to the gap in typical HTSC is of the order of tens of meV (e.g., the gap $2\Delta\simeq 30$ meV for YBaCuO).

The interaction between optical radiation and a superconductor is presented in Fig. 10.[65] Photons incident on a superconductor break Cooper pairs and generate quasiparticles with energies $E\gg 2\Delta$ (see Fig. 10a). Electrons possessing such high energies relax very rapidly (through electron–electron and electron–phonon collisions) to states with energies in the range of the gap energy (see Figs. 10b and c). An absorption of a photon generated a large number of quasiparticles and phonons in the range of energy gap during a very short period of time (see Fig. 10d). The recombination of excited quasiparticles is accompanied by the creation of Cooper pairs and emission of phonons (see Fig. 10e). Pair breaking by phonons with energies $>2\Delta$ occurs during the characteristic time τ_B (see Fig. 10f). Over the time τ_{es}, phonons escape from the film to the substrate (see Fig. 10g). Other processes with their own characteristic times also exist, including the scattering of excited quasiparticles accompanied with absorption (see Fig. 10h) or emission (see Fig. 10i) of a phonon. The time of energy relaxation of electrons through the electron–phonon interaction is an important parameter characterizing the intensity of this interaction.

Nonequilibrium effects in HTSC materials are mainly observed in structures with Josephson properties (bridges and junctions in edge steps as well as bicrystalline sub-

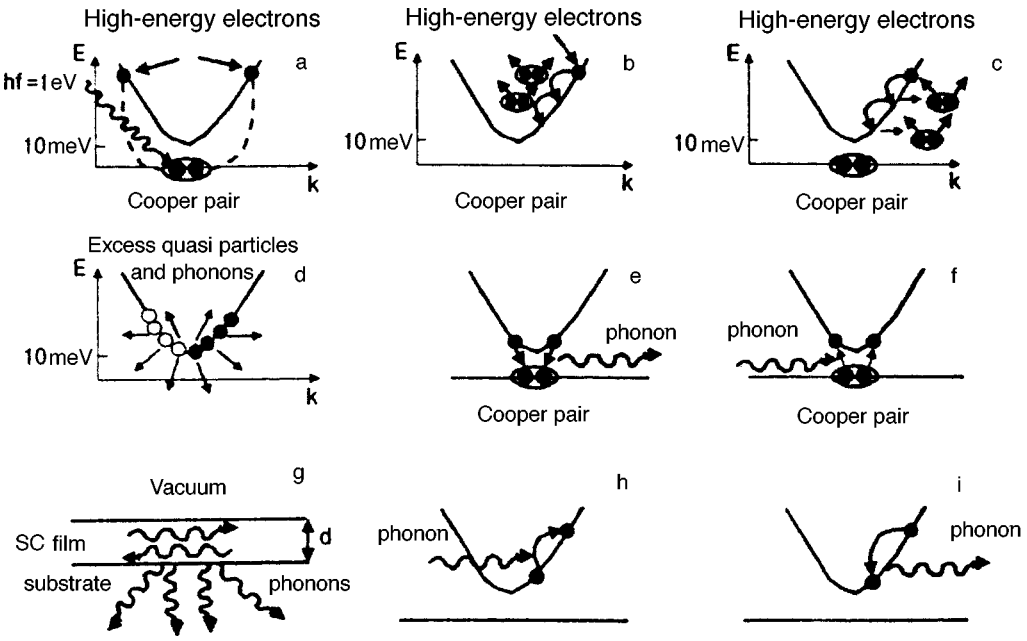

FIG. 10. Interaction between photons, quasiparticles, and phonons in superconductors (see the text) (from Gilabert[65]).

strates). In spite of considerable technological difficulties associated with a small length ξ in HTSC materials, Josephson structures with quite reproducible properties, such as junctions at edge steps, can be obtained even now by using various artificial approaches. Sometimes, the region of a weak link in such structures is coated by a photoconducting layer (usually CdS) in order to improve the sensitivity of the detector and to prevent the degradation of the sample.[65]

Enomoto *et al.*[68] studied the response of thin ($\sim 0.2\ \mu$m) BaPbBiO films ($T_c = 13$ K) to IR radiation. It is well known that the critical current of JJ is determined by the Ambegaokar–Baratov relation $I_c = \pi\Delta/(2eR)\tanh(\Delta/2k_BT)$, and at $T \ll T_c$ we have $I_c \approx \pi\Delta/2eR$. Irradiation of the superconductor leads to a change in the critical current $\delta I_c \approx (\pi\delta\Delta)/2eR$, where the change in the energy gap is connected with the number of excess quasiparticles through the relation $\delta\Delta = \delta n/N(0)$. Thus, knowing the change in critical current, we can find the change in the energy gap and the number of excess quasiparticles. Figure 11 shows schematically the IVC for a tunnel JJ exposed to radiation and without it. In the RSJ model, the IVC of a weak bond is described by the formula[65]

$$V = R(I^2 - I_c^2)^{1/2}. \tag{21}$$

This leads to the following expression for the photoresponse of the weak coupling:

$$\Delta V = -\frac{RI_c\delta I_c}{(I^2 - I_c^2)^{1/2}} = \frac{-\pi I_c\delta\Delta}{2e(I^2 - I_c^2)^{1/2}} \quad \text{for } I > I_c \tag{22}$$

and

$$(\Delta V)_{I=I_c} = R(2I_c\delta I_c)^{1/2} = \frac{\pi}{e}(\delta\Delta/2)^{1/2} \quad \text{for } I \leqslant I_c. \tag{23}$$

The variation of the IVC for a weak link under radiation is shown in Fig. 12a, and the response as a function of bias current together with the dependence calculated by formulas (21)–(23) is presented in Fig. 12b.

Later, Tanabe *et al.*,[69] who studied the response of bridges made of thin YBaCuO and LaSrCuO films to pulsed optical radiation ($\Lambda \sim 1.3\ \mu$m), detected a fast component in the response. The dependence of the response voltage ΔV on I_b had a peak which became narrower and higher upon cooling. With increasing I_b, the peak on the temperature dependence of the response increased and shifted to lower temperatures. The responsivity for the nonbolometric response associated with pair breaking is described by the formula

$$R_{NE} = \left.\frac{\delta V}{\delta I_c}\right|_{I_c} \left.\frac{\delta I_c}{\delta\Delta}\right|_T \left.\frac{\delta\Delta}{n_{qp}}\right|_T \frac{\delta n_{qp}}{P}, \tag{24}$$

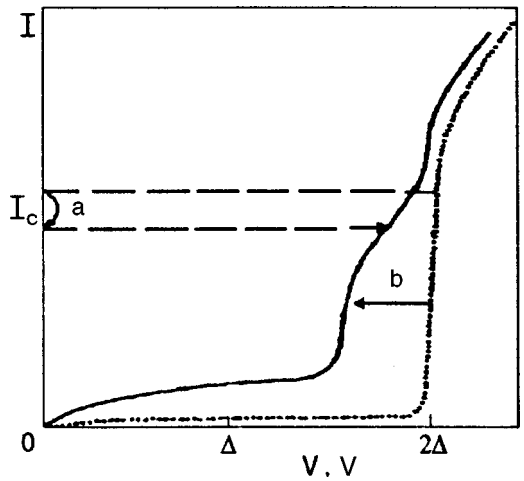

FIG. 11. Typical IVC of a Josephson tunnel junction. Solid and dashed curves represent IVC with irradiation (a) and without it (b) (from Gilabert[65]).

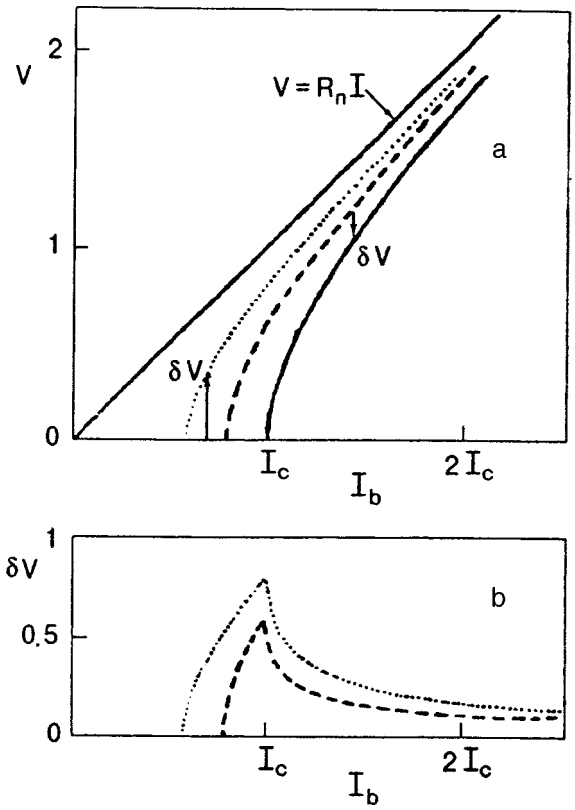

FIG. 12. Effect of radiation on a weak link: the solid curve corresponds to IVC in the absence of radiation, while the dashed and dotted curves correspond to irradiation (a); dependence of the voltage shift δV on the bias current I_b for two characteristics $V(I)$ (dotted and dashed curves) (b) (from Gilabert[65]).

where n_{qp} and P are the number density of quasiparticles and radiation power respectively. The first cofactor in (24) defines the dependence on the bias current I_b, while the temperature dependence is presented by the second and fourth cofactors. The third cofactor can be expressed in terms of the density of states N as $\delta\Delta/\delta n_{qp}=1/2N(0)$. The second cofactor follows the temperature dependence of the critical current, which determines the general temperature dependence of the response. Consequently, the overall temperature dependence is mainly determined by the dependence $I_c(T)$, which was just observed by Tanabe *et al.*[69] According to Tanabe, the value of responsivity is mainly determined by the cofactor $N(0)\Delta/2$. The experiments with YBaCuO and LaSrCuO films give the value of responsivity $\sim$20–30 V/W at low temperatures ($\sim$5 K), while the value of responsivity for similar BaPbBiO films is two orders of magnitude higher. The authors explain this by a considerable difference in the population densities for these two classes of superconductors and assume that the breaking of Cooper pairs by radiation is the basic mechanism of the response.

Johnson[70] studied thin YBaCuO films (20–200 nm) with high values of J_c ($>10^5$ A/cm^2) in quasi-two-dimensional geometry. The response to optical radiation ($\Lambda\simeq 665$ nm) with a pulse duration 0.3 ps and pulse repetition frequency 2 kHz was recorded with the help of ultrahigh-speed oscillograph (10 ps$<t<$10 ns). It was found that the response contains two component: in the vicinity of $T_c\pm\Delta T/2$ (where $\Delta T=3$ K is the superconducting transition width), a bolometric signal with a time constant $\sim$3 ns was observed, which increases linearly with the bias current I_b as well as with the radiation power. The second component observed at $T<T_c-\Delta T/2$ has a fall time $\sim$100 ps and is characterized by a steeper than linear dependence on P and I_b with saturation for large values of the argument. In spite of the fact that the position of the peak on the low-temperature component was exactly the same as for the peak of dR/dT, the response was almost two orders of magnitude stronger than the bolometric signal and was virtually independent of temperature at low temperature for which $dR/dT\to 0$. Besides, the response decreased with time much more rapidly ($\sim$100 ps) than the bolometric component ($\sim$3 ns) at $T>T_c-\Delta T/2$. Johnson drew the conclusion that the observed response is associated with photoinduced breaking of Cooper pairs.

A nonbolometric response was also observed by some authors in HTSC epitaxial films.[71] The optical response in the femtosecond range studied with the help of the ''pump–probe'' method (see Sec. 1) demonstrated the avalanche multiplication of quasiparticles following the absorption of a photon.[14] This process is associated with inelastic electron–electron scattering on the time scale $\tau_{ee}\leqslant 1$ ps. Quasiparticles also interact with phonons through inelastic electron–phonon scattering. This loss mechanism is associated with the energy gap suppression as well as with the motion of vortices. A decrease in the number density of Cooper pairs also leads to a change in the kinetic inductance, which also affects temporal characteristics of the response.[72]

Han *et al.*[73] studied the dynamics of a femtosecond response in YBaCuO films of thickness 100–500 nm on a $SrTiO_3$ substrate. They used a laser with a pulse duration $\sim$60 fs, $\Lambda=625$ nm, and the pulse repetition frequency 80 MHz. The typical shape of transient response signal at $T>T_c$ and $T<T_c$ is shown in Figs. 13a and 13b respectively. In the normal state, the response ΔR is positive. It emerges abruptly during the time $\sim$1 ps and decreases slowly over $\sim$3 ns. A comparison of the response with dR/dT revealed its bolometric origin. At the same time, the transient response is negative at $T<T_c$ with a rise time $\sim$300 fs and with a rapid fall to zero over 7–8 ps. After this the response becomes positive due to the thermal effect associated with diffusion of phonons (in analogy with the response at $T>T_c$). It was found that the temperature dependence of the peak height of the response is successfully approximated by the two-fluid model and has the form $[1-(T/T_c)^4]$. Han *et al.*[73] proposed that the optical response mechanism includes the two main processes: (1) avalanche multiplication of quasiparticles following the absorption of a photon, and (2) nonlinear recombination of photogenerated quasiparticles. Han *et al.*[73] also noted that the quasiparticle response is observed only when the system is not saturated. Indeed, the maximum number density of photoinduced quasiparticles estimated from the data on radiation intensity proved to be an order of magnitude smaller than the characteristic density of states in HTSC materials ($N_s\sim 10^{21}$ cm^{-3}). The authors of Ref. 73 also noted that the recombination rate v increases slightly in the interval from 0 to $T_c/2$ and then decreases rapidly. This is explained by the fact that the recombination

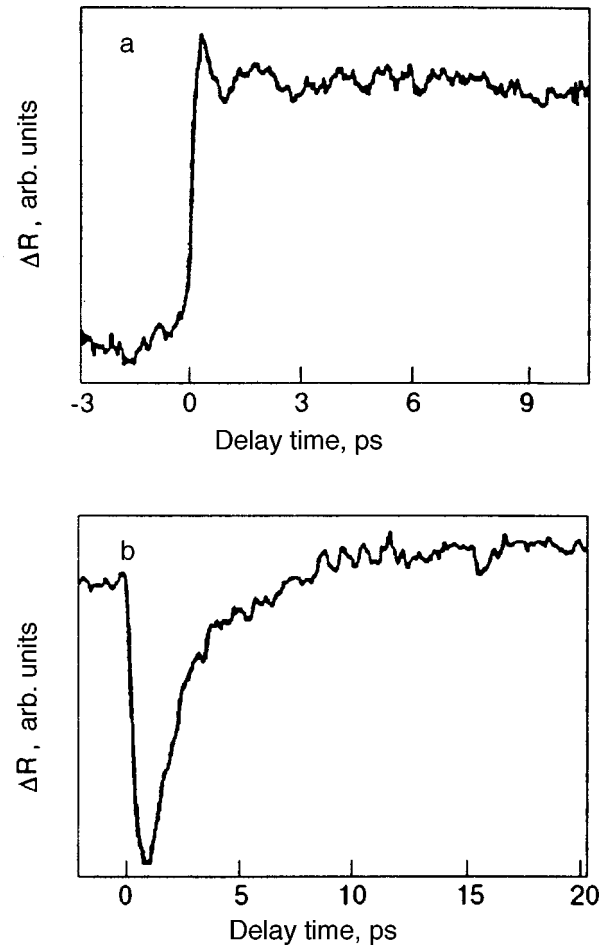

FIG. 13. Transient response ΔR of an epitaxial YBaCuO film at $T=300$ K (a) and 20 K (b) ($T_c=93$ K) (from Han *et al.*[73]).

of quasiparticles is accompanied by the generation of optical phonons that interact resonantly with the gap. The latter circumstance leads to a decrease in the gap width and to softening of this resonant interaction. The decrease in the gap width in turn is manifested directly in a decrease in the recombination rate.

Analyzing the femtosecond dynamics of the optical response, Sobolewski *et al.*[15] proved that the response of YBaCuO epitaxial films of thickness 80–250 nm has a characteristic time ~30 ps and can be explained in the thermomodulation model according to which hot holes are generated by radiation. A redistribution of these holes leads to a displacement (rise) of the Fermi level E_F in copper–oxygen planes, resulting in the emergence of a response. A decrease in the oxygen concentration in the film lowers E_F. If the energy of a probing radiation quantum is lower than the Fermi level (in the initial state), the value of E_F increases upon irradiation. The polarity of the response signal must change at the instant of crossing the energy level corresponding to the energy of the beam, which was actually observed by Sobolewski *et al.*[15] and by Han *et al.*[73] (see Figs. 13a and 13b). If, however, the value of E_F is initially higher than the energy of the beam, the polarity of the response remains unchanged (positive; see Fig. 13a). Sobolewski *et al.*[15] emphasize that the application of the thermomodulation model

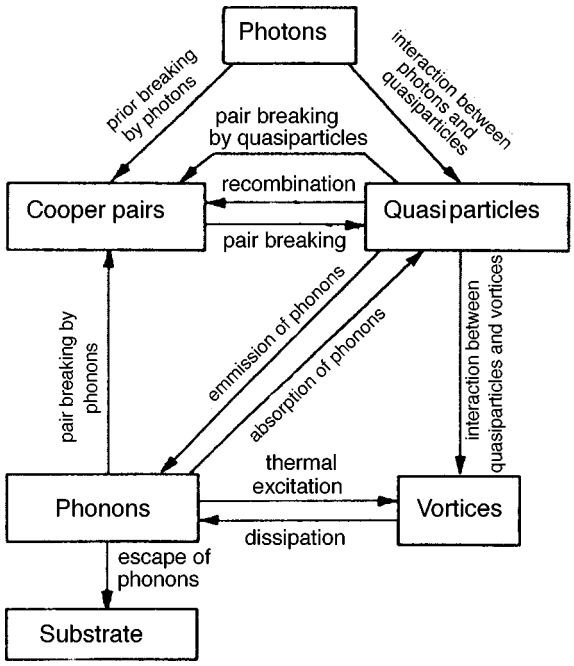

FIG. 14. Nonequilibrium processes in a superconducting film (from Zhang and Frenkel[72]).

is justified only for $YBa_2Cu_3O_{6+x}$ with the oxygen concentration $x>0.4$.

It should be stressed that vortices in type II superconductors, can also be involved in the optical response dynamics in addition to quasiparticles and phonons. The block diagram illustrating all possible types of interactions between these three subsystems is shown in Fig. 14. The processes occurring in the superconductor in this case can be explained as follows[72]: (1) photons interact with Cooper pairs and quasiparticles, generating electrons having a higher energy (the photon–electron interaction occurs during a time ~1 fs); (2) high-energy quasiparticles continuously break new Cooper pairs and generate extra quasiparticles during the time τ_{ee}; (3) quasiparticles interact with phonons through the absorption and emission of phonons ($\tau_{e\mathrm{ph}}$); (4) high-energy phonons break Cooper pairs (τ_B); (5) quasiparticles recombine into Cooper pairs and generate phonons (τ_B); (6) quasiparticles and phonons activate the motion of vortices, leading to dissipation (the corresponding time scales of these processes are denoted by τ_{ev}, $\tau_{\mathrm{ph}v}$, and τ_d); (7) phonons escape from the film to the substrate over the time τ_{es} of the order of nanoseconds.

According to Anisimov *et al.* and Qui and Tien,[74] the electron and phonon subsystems can be assumed to be in equilibrium with each other. The effective temperatures of the electron and phonon gases are given by[75]

$$C_e\frac{dT_e}{dt}=\kappa_e\nabla^2T_e-\gamma_{e\mathrm{ph}}(T_e-T_{\mathrm{ph}})-\gamma_{ev}(T_e-T_0)+q_{ab} \tag{25}$$

and

$$C_{\mathrm{ph}}\frac{dT_{\mathrm{ph}}}{dt}=\kappa_{\mathrm{ph}}\nabla^2T_{\mathrm{ph}}+\gamma_{e\mathrm{ph}}(T_e-T_{\mathrm{ph}})$$

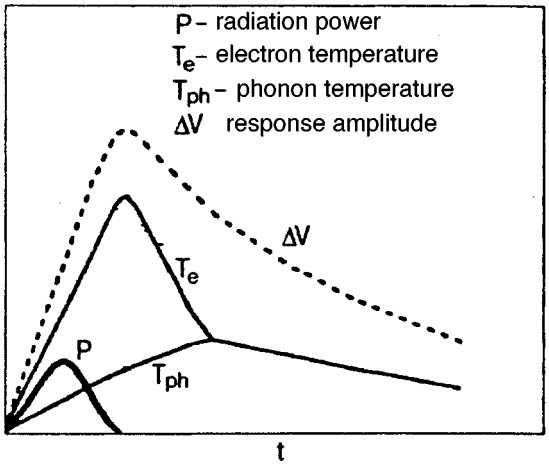

FIG. 15. Time evolution of radiation power P, effective electron (T_e) and phonon ($T_{\rm ph}$) temperatures, and the signal amplitude ΔV of the response of a superconductor to optical radiation (from Zhang and Frenkel[72]).

$$-\gamma_{{\rm ph}v}(T_{\rm ph}-T_0)+q_d\,. \tag{26}$$

where T_e and $T_{\rm ph}$ are effective temperatures of electrons and phonons, T_0 is the equilibrium temperature before irradiation, C_e and $C_{\rm ph}$ are heat capacities per unit volume, and κ_e and $\kappa_{\rm ph}$ the thermal conductivities of the electron and phonon subsystems respectively, $\gamma_{e{\rm ph}}$, γ_{ev}, and $\gamma_{{\rm ph}v}$ are the electron–phonon, electron–vortex, and phonon–vortex coupling constants respectively, and q_{ab} and $q_{\rm d}$ are the absorbed and scattered power densities. The solution of this system of equations makes it possible to calculate the enhancement in the electron temperature relative to the phonon temperature as a result of irradiation. When the duration of radiation pulse is $\tau \geqslant \tau_{e{\rm ph}}$, the electron temperature approaches the phonon temperature. For $\tau \gg \tau_{ee}$ and $\tau_{e{\rm ph}}$, the effective temperatures of electrons and phonons are approximately equal. Figure 15 shows the dynamics of the most important characteristic times as well as the input pulse, when the duration of the latter is shorter than the electron–phonon relaxation time. It can be seen that the value of T_e attains the peak at the end of optical pulse, and the peak of the response corresponds to the peak of T_e. According to Frenkel,[75] the thermal relaxation time determined by the time $\tau_{\rm es}$ during which phonons escape to the substrate can be reduced by eliminating the resistance of the ''film–substrate'' thermal interface by using narrow superconducting microstrips as detectors. The sensitivity in the bolometric mode can be improved by enhancing pinning in operation with large bias currents. However, the mechanisms of interaction between electrons and vortices, phonons and vortices, as well as vortex dissipation have not been studied completely so far.

Gol'tsman *et al.*[7] studied the response of YBaCuO films prepared by laser ablation on various substrates to pulsed ($\tau \sim 20$ ps) optical ($\Lambda = 0.63$ and 1.54 μm) radiation with a pulse repetition frequency 0.5 Hz. The time dependence of transient response has the form of a solitary pulse with steep left slope (of the order of several ps) corresponding to the nonequilibrium component and a ''smeared'' (tens of ps) right slope corresponding to the bolometric component (Fig. 16). The peak of the response amplitude corresponds to the

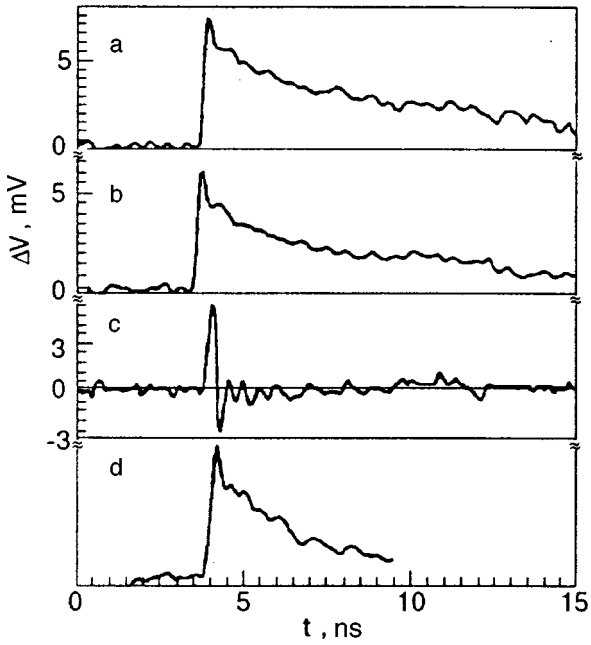

FIG. 16. Transient response of a YBaCuO microbridge at various temperatures (a–c): $T = 100$ K (normal state, $I_b = 7.5$ mA, $E = 40$ μJ/cm^2) (a); $T = 85$ K (near the middle of the junction, $I_b = 1$ mA, $E = 2$ μJ/cm^2) (b); $T = 54$ K (superconducting state, $I_b = 1$ mA, $E = 40$ μJ/cm^2) (c); the integral of the curve in Fig. 16c with respect to time (d) (from Gol'tsman *et al.*[7]).

steepest part of the superconducting transition. The shape of the right slope first followed an exponential law, and then a power law identified with a rapid bolometric effect and thermal diffusion to the substrate. Since the time constant corresponding to the exponential decay is proportional to the film thickness, Gol'tsman *et al.*[7] explain this process by the escape of nonequilibrium phonons to the substrate. When nonequilibrium phonons return to the film, a transition from the rapid bolometric effect to diffusion flow with power attenuation takes place. As the temperature decreases ($T = 54$ K), the ratio of the amplitudes of fast and slow components increases, and a signal with negative polarity is formed simultaneously. The response integrated with respect to time is exactly similar to the response in the normal and resistive states, but is characterized by a larger ratio of the amplitudes of the fast and slow components (Fig. 17).

A similar behavior is observed in the dependence of the response shape in the superconducting state on the displacement current at constant temperature. At first ($I_b = 2$ mA), the negative component decreases, and then vanishes altogether, while the positive component appears. For large values of $I_b (\sim 10$ mA), the wavy shape of the response resembles that in the resistive and normal states. The authors draw the conclusion that a nonequilibrium picosecond component is observed in all the three states. In the normal state, photoexcited charge carriers possess a lower scattering rate than in the equilibrium state, which leads to a decrease in the mobility of charge carriers and hence to an increase in resistance. In the superconducting state, the nonequilibrium response is associated with a change in kinetic inductance. However, in the resistive state (in the superconducting transition region), the inductive and resistive components coex-

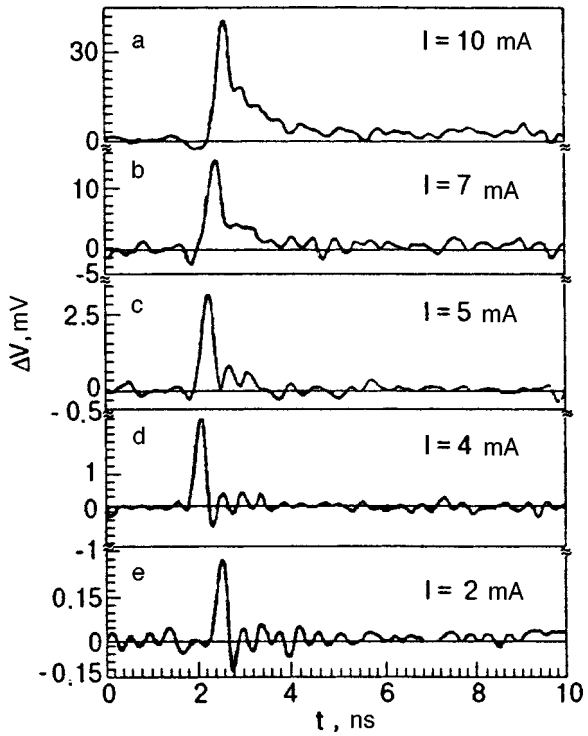

FIG. 17. Transient photoresponse of a YBaCuO microstrip line at $T=4.2$ K, $E=2$ μJ/cm^2 and various bias currents I_b, mA: 10 (a), 7 (b), 5 (c), 4 (d), and 2 (e) (from Gol'tsman *et al.*[7]).

ist. It was also found that the ratio of the amplitudes of the nonequilibrium and rapid bolometric components virtually does not change during a transition from the normal to the superconducting state. This means that none of superconducting peculiarities affects the shape of a transient pulse, and only the magnitude of the nonequilibrium component commensurate with the bolometric component is affected. This feature is typical of the effect of suppression of the gap by excess quasiparticles generated by irradiation, which results in an increase in resistance in the normal and resistive states or an increase in the kinetic inductance in the superconducting state. This effect is responsible for the coexistence of the nonbolometric and fast bolometric mechanisms in the normal, resistive, and superconducting states of YBaCuO epitaxial films.

Heusinger *et al.*[8] studied NbN films in the form of multistrip structures (having a length of 140 μm and a width of 0.8 μm separated by 3.2 μm on sapphire substrates. Separate strips made of YBaCuO epitaxial films of thickness 80 μm, length 800 μm, and width 80 μm were placed between contact areas. Both types of superconductors in the superconducting state exhibit a bipolar response to pulsed (100 fs) optical radiation with a wavelength of 0.8 μm and a pulse repetition frequency up to 82 MHz. The positive peak of the response for NbN had the rise and fall time $\sim$40 ps and preserved its duration in the entire temperature range 20 K $<T<T_c$. It was followed by a negative peak with a fall time $\sim$190 ps, which broadened with increasing temperature. According to Heusinger *et al.*[8] this peak reflects relaxation processes in the film. For all values of bias current I_b (up to 0.3 mA) and integral power density P_l (up to 0.6 mJ/cm^2), the photoresponse preserved its shape, and its amplitude was proportional to I_b and P_l. For YBaCuO samples, the duration of the positive and negative peaks of the response was $\sim$25 ps and $\sim$35 ps, respectively. The amplitude of the response on the whole was proportional to the bias current. At the same time, the response in the superconducting transition region was formed by a bi-exponential unipolar voltage peak which is correctly described in the two-temperature model.[71] According to Semenov *et al.*,[71] the mechanism of the response away of the transition is associated with nonequilibrium change in the kinetic inductance of the superconductor under radiation, while the shape and amplitude of the response are determined by the temperature evolution of the number density of Cooper pairs. This is confirmed by good agreement between experimental results and the theory developed in Ref. 71, which gives a relation between the response voltage and the change dN_{sc} in the number density of pairs under irradiation. It is assumed that the working temperature should be maintained below T_c (away from the transition temperature) to optimize the speed of response of a detector based on the given effect since the signal has no slow ''tail'' characteristic of the resistive state at low temperatures.

Salient features and conditions for realization of the mechanism

(1) Depending on temperature, the response is almost constant at low temperatures and decreases abruptly as T_c is approached.
(2) The response associated with the breaking of Cooper pairs appears at lower threshold levels of the signal as compared to the bolometric component, has much higher speed (10–100 ps), and is characterized by clearly manifested saturation as a function of radiation intensity.
(3) The temperature dependence of the response at low temperatures is either exponential, or coincides with the temperature dependence of critical current (for $h\nu>2\Delta$ and for large deviations from equilibrium).
(4) The amplitude of the response increases sharply with the bias current (more steeply than linear dependence) and attains saturation for large I_b.

2.6. Electron heating

The idea of a bolometer based of the effect of electron heating in superconductors was put forth for the first time at the beginning of eighties by Gershenzon *et al.*[76] These authors divide all nonequilibrium effects into two large categories: Josephson and electronic detection mechanisms (JDM and EDM). The idea lies in electron heating by radiation with phonons as a thermostat. Such a mechanism can exist when the heat capacity of the phonon subsystem is higher than that of the electron subsystem: $C_{\rm ph}/C_e>100$.[76] The EDM was realized in practice only in two cases.[77] In one case, it was associated with granular BaPbBiO films at $T \ll T_c(T_c=13.6$ K). The radiation suppresses the order parameter in granules, which is accompanied by a decrease in the critical current of intergranular weak links and the emergence of additional resistance in the resistive state of weak links.[68] The search for this mechanism in HTSC materials

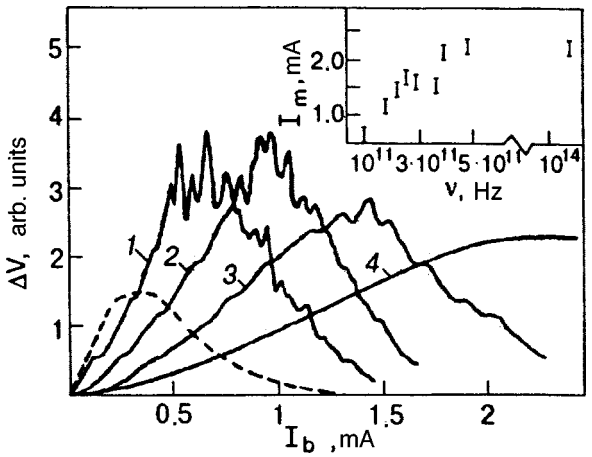

FIG. 18. Dependence of the response ΔV on the bias current I_b for a YBaCuO film for various radiation wavelengths Λ, mm: 2.2 (curve *1*), 1.5 (curve *2*), 1.1 (curve *3*), 0.6 and 8×10^{-4} (curve *4*) and $B=0$ (solid curves) and 3 T (dashed curves), $T=4.2$ K. The inset shows the frequency dependence of the maximum response current I_m (from Aksaev *et al.*[77]).

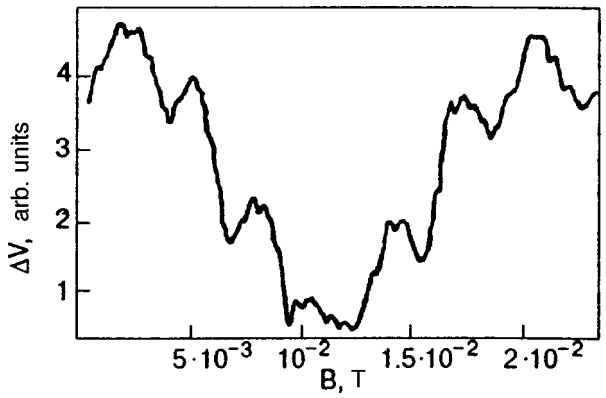

FIG. 19. Field dependence of oscillations of the response ΔV for a granular YBaCuO film at $T=4.2$ K, $\Lambda=2.2$ mm, $I=2\ \mu$A (from Aksaev *et al.*[77]).

did not lead to any positive results by the beginning of the nineties.[77] Another method of realization of EDM was investigated in detail for thin homogeneous Nb, Al, and NbN films.[76] The main difference between these results and those obtained in Refs. 68 is that superconductivity is suppressed considerably in the entire volume of the film, and the resistive state is attained due to transport current and/or magnetic field. The high concentration of quasiparticles as well as their small mean free path (due to scattering by defects) enhance the Coulomb interaction between quasiparticles. The latter is responsible for a lack of selectivity (absence of frequency dependence) of the heating mechanism. Indeed, high-intensity electron–electron interaction leads to an effective redistribution of absorbed energy in the electron subsystem, which is enhanced owing to secondary breaking of Cooper pairs by nonequilibrium quasiparticles and an increase in their number density. Cooling of the electron subsystem as a result of the electron–phonon interaction as well as recombination of quasiparticles turns out to be slower. The resistive state is characterized by a large steepness of dR/dT and serves as a sensitive indicator of electron heating: $\Delta V = I(dR/dT)\Delta\Theta$, where Θ is the effective electron temperature. The condition of phonon thermostat is observed for a small film thickness such that the time $\tau_{\rm es}$ of phonon escape from the film is shorter than the time $\tau_{\rm phe}$ of phonon-electron scattering. The time constant of the effect is determined by the electron–phonon relaxation time $\tau_{e\rm ph}$. In a narrow range in the vicinity of the superconducting transition $[\Delta(T, H)/k_BT \ll 1]$, the response relaxation time τ is associated with the dynamics of superconducting condensate and is equal to the order parameter relaxation time $\tau_\Delta \sim (k_BT/\Delta)\tau_{e\rm ph}$. A characteristic feature of electron heating is the increase in relaxation rate with temperature.

Aksaev *et al.*[77] studied bridges having a length of 0.01–4 mm and a width of 1–500 μm made of YBaCuO granular films of thickness 0.1–1 μm on Al_2O_3 and MgO substrates. All the samples under investigation could be divided into two categories: the films exhibiting typical features of JDM (A) and those in which EDM was manifested (B). The response was studied in a wide spectral range from $\Lambda=2.2$ to $8\cdot10^{-4}$ mm. The dependence of the response ΔV on bias current had the shape of a curve with a peak which was displaced towards higher values of I_b and became lower upon an increase in frequency. The $\Delta V(I_b)$ dependence for samples of group A had quasiperiodic peaks that ''smeared'' with increasing temperature, frequency, and magnetic field (Fig. 18). For radiation wavelengths $\Lambda<0.6$ mm, the $\Delta V(I_b)$ dependences coincides (curve *4* in Fig. 18 corresponds to $\Lambda=0.6$ and $8\cdot10^{-4}$ mm simultaneously). Similar suppression of peaks also took place at a fixed frequency upon an increase in radiation power. A finite voltage appears on the IVC for samples belonging to both groups (A and B) for infinitely small values of $I_b\geqslant0$, i.e., $I_c\simeq0$. According to Aksaev *et al.*,[77] this is due to a large spread in the parameter of weak links.

The magnetic field dependence of the response for samples of group A in the field range 10^{-2}–10^{-3} T is oscillating with two characteristic periods $\Delta B=4\cdot10^{-3}$ and $1.9\cdot10^{-2}$ T (Fig. 19). Such oscillations are not observed for samples of group B on $\Delta V(I)$ or $\Delta V(B)$ curves.

The dependence of the response on the amplitude modulation frequency is shown schematically in Fig. 20. It can be seen that at low temperatures, the decrease in response with

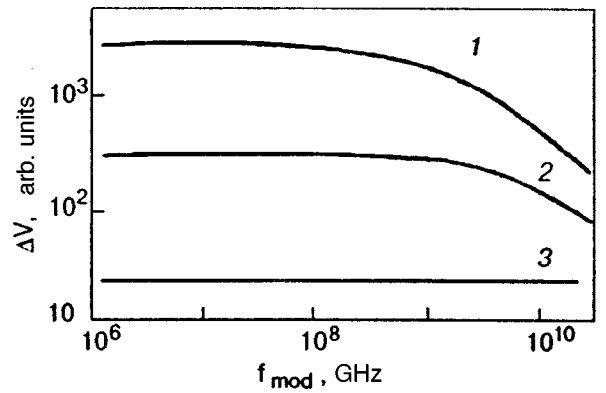

FIG. 20. Dependence of the response ΔV on the modulation frequency $f_{\rm mod}$ for a granular YBaCuO film with a constant impedance at various temperatures T, K: 1.7 (curve *1*), 4.2 (curve *2*) and 77 (curve *3*) (from Aksaev *et al.*[77]).

increasing frequency starts at lower frequencies, while the response at 77 K is constant over the entire frequency range under investigation (0.1–12 GHz). The frequency dependence of the response is described by the formula[77]

$$\Delta V(\nu)=\Delta V(0)[1+(2\pi\nu\tau)^2]^{-1/2}. \quad (27)$$

Using this expression and the experimentally obtained dependence $\Delta V(\nu)$ for various temperatures, the authors obtained the response time $\tau(T)\sim T^{-1}$ over the entire temperature range from 6 to 40 K. It was found that the value of τ does not depend on the substrate material or on the film thickness in the range 0.1–1 μm.

An analysis proved that samples of group A for which oscillations of $\Delta V(I_b)$ and $\Delta V(B)$ are observed display JDM: the peaks on the $\Delta V(I_b)$ curve (see Fig. 18) correspond to Shapiro steps on IVC, which are formed as a result of irradiation of weak intergranular links, while oscillations of ΔV in a magnetic field correspond to oscillations of I_c. The transverse (relative to current) size L of weak links can be estimated from the Josephson interference relation for critical current, i.e., $L=(h/8\pi e)\lambda_L\Delta B$, which gives $L=0.35$ and 1.7 μm (for $\lambda_L=2000$ Å). These values are in good accord with the actual size of microbridges.

As the radiation frequency increases, JDM is replaced by EDM due to electron heating in granules. This can be explained by spectral dependence of JDM sensitivity which varies in proportion to ν^2 for $\nu\sim 2\Delta/h$ in accordance with the theory (see Refs. 11, 24, 77). Since the heating effect remains independent of frequency, upon an increase in temperature, magnetic field, and with decreasing share of granular structure in the films, the frequency of crossover separating these two mechanisms decreases.

Samples of group B were distinguished by a lower degree of granulation and a larger thickness of intergranular junctions. The absence of JDM in group B samples is confirmed by the coincidence of the dependences $\Delta V(I)$ and $dV/dT(I)$, which is typical of the bolometric response. However, the estimates of the EDM time constant give 1–10 ps, which is one or two orders of magnitude smaller than the minimum possible time for a bolometric response defined by the parameter $\tau_{es}=4d/\eta c_s\simeq 10^{-10}$ s, where c_s is the velocity of sound. Besides, the observed response does not depend on the film thickness and the substrate material, which is also typical of a bolometric response. The optimization of EDM is possible for a choice of bias current for which weak links have already been broken, while granules are still in the superconducting state. The resistance at the working point usually amounts to $\sim$10% of the resistance R_n in the normal state. The form of the dependence $\tau(T)\sim T^{-1}$ suggests that the temporal characteristics of EDM are determined by $\tau_{e\text{ph}}$ rather than by the recombination time τ_R of quasiparticles in granules (excluding the temperature region near T_c), which is characterized by an exponential increase upon cooling. A similar dependence for LTS materials has the form $\tau(T)\sim T^{-2}$ corresponding to the temperature dependence of time $\tau_{e\text{ph}}$ in the normal state measured by other methods.[77]

The spectral characteristic of EDM is determined by the frequency dependence of the absorption coefficient α and of the change in the energy gap width $\delta\Delta^*$ ($\delta\Delta^*$ is the mean value of Δ in the resistive state). It is well known that the value of α for YBaCuO changes significantly in the near IR range even in the normal state, leading to a smooth decrease in ΔV with increasing frequency in this range. The absence of singularities in the response for $h\nu=2\Delta$ is associated with considerable inhomogeneity of the resistive state. The ratio of ΔV to the power P_A absorbed by unit volume remains unchanged in a wide frequency range, but was very sensitive to the mechanism of electron energy relaxation. Since the electron–electron interaction dominates in the case of a small mean free path l, energy is redistributed in the electron subsystem, excess quasiparticles are generated, and superconductivity is suppressed effectively for any frequency ν. Besides, the lower value of the Fermi energy in HTSC materials as compared to LTS substances confirms the effectiveness of the electron–electron interaction (along with the electron–phonon interaction), which explained the nonselective nature of the ratio $\Delta V/P_A$.

For $\nu>\tau_{e\text{ph}}^{-1}$, the response under the electron heating conditions is described by the formula[77]

$$\Delta V=(dV/dT)P_A\tau_{e\text{ph}}[1+(2\pi\nu\tau_{e\text{ph}})^2]^{-1/2}C_e^{-1}, \quad (28)$$

which can be used for deriving the temperature dependence of $\tau_{e\text{ph}}$ even in the temperature range inaccessible for measurements. According to (28), $\tau_{e\text{ph}}\sim T\Delta V(dV/dT)^{-1}$ for $\nu\ll(2\pi\tau_{e\text{ph}})^{-1}$ and $C_e=\gamma T$. It was found that the temperature dependences of τ calculated by formula (27) obtained from quasistationary measurements coincide with the dependence of $\tau_{e\text{ph}}$ calculated by formula (28) obtained from nonstationary measurements: both times are proportional to T^{-1}. This confirms the uniform nature of energy relaxation and indicates that diffusion of quasiparticles does not play any significant role in relaxation processes. Moreover, the smallness of the film thickness (as compared to λ_L), which ensures a uniform absorption of radiant energy, is an important condition for realization of electron heating.

Lindgren *et al.*[5,6] studied the response of microbridges made of YBaCuO epitaxial films of thickness 100 nm on $LaAlO_3$ substrates to optical radiation with $\Lambda=790$ nm, pulse duration 100 fs, and pulse repetition frequency 76 MHz. A bridge having the size 5×7 μm was placed at the center of a coplanar waveguide of length 4 mm and width 30 μm through which a bias current of frequency $\sim$18 GHz was supplied via a semirigid coaxial cable. The entire sample was coated with a layer of $LiTaO_3$ insulating crystal to facilitate electro-optical measurements made in the ''pump–probe'' technique (see Sec. 1). The incident beam was focussed in the region of the bridge while the probing beam was focussed at a distance of $\sim$20 μm from the bridge in the region of insulating gap. The sample heating estimated from the absorbed power was $\sim$0.2 K.

The current-voltage characteristics of HTSC samples were measured by the four-probe technique in the temperature range 20–80 K. The IVC were characterized by two clearly distinctive voltage modes: the superconducting state (flux flow with zero/low voltage across the bridge) and the resistive state in which the current is almost constant, while the voltage increases abruptly (Fig. 21). With increasing bias current, a transition occurs from the superconducting state to

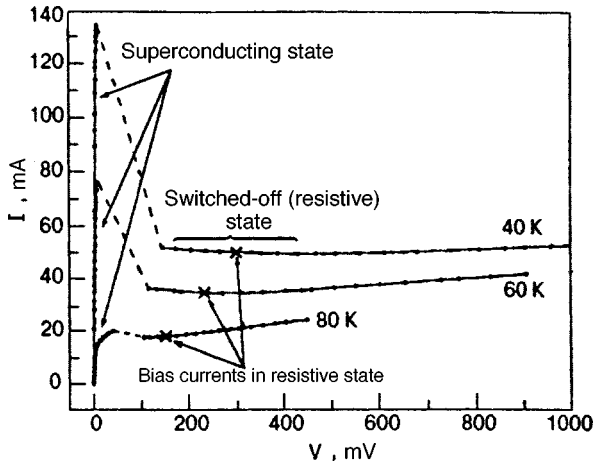

FIG. 21. Current-voltage characteristic of a YBaCuO microbridge measured by the four-probe technique (from Lindgren *et al.*[6]).

the flux flow regime in which the bridge becomes dissipative (dissipates heat). The hot spot increasing with a further increase in I_b gradually transforms the bridge to the resistive state with a low and direct current and a high voltage. In the hot spot region, the temperature is maintained at a nearly constant level exceeding T_c. At still higher values of I_b, the bridge goes over to the normal state, and the IVC becomes linear.

In the resistive state, a transient response has the form of a narrow solitary pulse having a width ~ 1.1 ps at half height in the entire temperature range 20–80 K. The response was followed by a voltage plateau (~ 200 μV) associated with a slow bolometric response with a nanosecond fall time (Fig. 22).

According to the model of photoinduced nonequilibrium electron heating, the rise time for a transient pulse is determined by the larger of two time intervals, i.e., the duration of the laser pulse or by the time τ_{et} od electron thermalization. Since the laser pulse in this case is shorter, and hence does not limit the evolution of the nonequilibrium processes under consideration, Lindgren *et al.*[5,6] who used the model of electron heating managed to determine from the results of measurements the two fundamental characteristics of the samples, viz., the electron thermalization time $\tau_{et} \simeq 0.56$ ps and the electron–phonon relaxation time $\tau_{eph} \simeq 1.1$ ps.

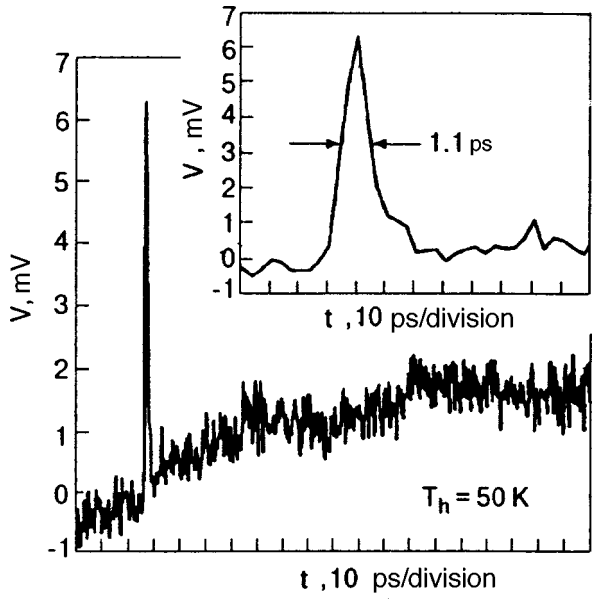

FIG. 22. Transient response of a YbBaCuO bridge in the resistive state at $T_b = 50$ K. Nonzero initial level is due to slow drift of the scanning beam relative to the center of the gap between coplanar waveguides (from Lindgren *et al.*[6]).

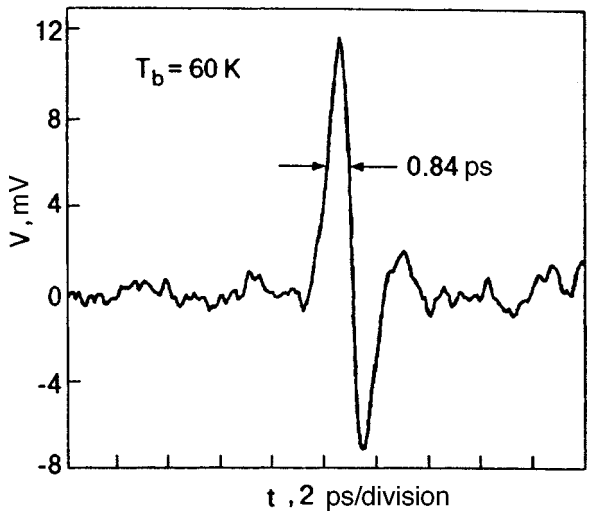

FIG. 23. Transient response of a YbBaCuO bridge in the superconducting state at $T_b = 60$ K (from Lindgren *et al.*[6]).

In the superconducting state (for small bias currents), a bipolar shape of the response is observed (Fig. 23) with a time constant ~ 1 ps typical of the kinetic inductance mechanism. Additional experiments with the removal of the probing beam to a distance ~ 600 μm from the bridge demonstrated a considerable decrease in amplitude and distortion of the shape of the transient response pulse.[6] Lindgren *et al.*[6] believe that it was the distortion of the shape of a pulse propagating along the transmission line from the bridge to the region of recording, which was observed in early experiments led to erroneous interpretation of the response mechanism as a change in kinetic inductance as a result of uniform heating of the entire region of the bridge. For this reason, the response should be measured as closely to the bridge as possible to reduce pulse distortion effects. Lindgren *et al.*[6] assumed that in this case a nonequilibrium change in the kinetic inductance $L_{\rm kin}$ takes place, in which the variation of the relative fraction of condensate is associated with the electron temperature T_e rather than with the temperature T_b of the thermostat. Lindgren *et al.*[6] attained excellent agreement between the experimental shape of the response in the resistive state and the two-temperature model.[71] The rise time for electron temperature $\tau_{et} = 0.56$ ps and the fall time $\tau_{\rm eph} = 1.1$ ps were extracted from the approximation of experimental data. Since both times exceed the laser pulse duration, they are regarded as intrinsic characteristic times for photoresponse in YBaCuO. The application of the kinetic inductance model described in Ref. 6 leads to an equally good agreement with experimental results in the superconducting state. This made it possible to determine the rise time

of the response $\tau_{et}=0.9\pm0.1$ ps which virtually remains unchanged in the temperature range 20–80 K. This value is much larger than $\tau_{et}=0.56$ ps in the resistive state. The negative component of the response was approximated by using the value of $\tau_{e\text{ph}}=1.1$ ps obtained from measurements in the resistive state and was found to be in satisfactory agreement with experimental data. The linear dependence of the response on I_b also confirmed the effectiveness of the kinetic inductance mechanism.

As regards applications, the kinetic inductance mode is less interesting[6] in view of the oscillatory form of the response. At the same time, the observed effect of optically induced electron heating can be used for developing high-speed detectors and mixers with an intermediate frequency band above 100 GHz in the range from infrared to ultraviolet radiation. Such photodetectors can also be used in fiber optical transmission lines with a data transmission rate >100 Gbit/s. Another region of application can be high-speed optoelectrical transducers using high-speed single flux-quantum circuits and optical fibers for high-speed data transmission.

Salient features and realization conditions for the mechanism

(1) Thin HTSC films can exhibit both Josephson and electronic monitoring mechanisms, a transition from the former to the latter occurring upon an increase in frequency. With increasing temperature, magnetic field, and radiation power, the value of transition frequency decreases. Besides, this frequency is the lower, the smaller the degree of granulation and the larger the grain size in the film. For films with a granule size ~1 μm at 4.2 K and low radiation powers, the transition region lies in the submillimeter range.
(2) For the realization of EDM, the film thickness must be smaller than the radiation penetration depth.
(3) The inertia of the response is determined by the time $\tau_{e\text{ph}}$ of the electron–phonon relaxation, which decreases upon an increase in temperature in proportion to T^{-1}.
(4) The EDM is characterized by the lack of selectivity in a wide frequency range, high values of responsivity (10^3–10^5 V/W), and a low noise level ($P_{\text{eq}}\sim10^{-12}$–$10^{-14}$ $W/\text{Hz}^{1/2}$).[76]

2.7. Percolation superconductivity

This mechanism of response was proposed for the first time by Afanasyev *et al.*[78,79] who studied the interaction between EMR of the millimeter range and thin YBaCuO films. The same authors[80] studied the response of three different YBaCuO films to mm radiation: (1) multiphase granular film (of thickness $d\simeq1$ μm), (2) polycrystalline film with a granule size ~1 μm ($d\simeq1$ μm) and (3) epitaxial film ($d\simeq0.1$ μm). For film 2, two peaks were observed on the temperature dependence of the response, one of which coincided with the dR/dT peak, while the other was manifested in the region of resistive tail. The epitaxial film had only one high-temperature (bolometric) peak, and a weak low-temperature component was observed only for very large bias currents ($I_b\geqslant10$ mA). For film 1, only the low-temperature component was observed for any attainable I_b, which increased in amplitude and was displaced towards low temperatures with increasing I_b. A comparison of the dependences $\Delta V(I_b)$ and $d^2V/dI^2(I_b)$ proved that the response is not associated with an ordinary monitoring mechanism due to nonlinearity of IVC.[79] The low-temperature component for film 2 behaved in the same way as for film 1, while the high-temperature component increased in proportion to I_b. The application of a weak magnetic field caused oscillatory behavior of the resistance $R(H)$ and $\Delta V(H)$ typical of JJ at temperatures corresponding to the low-temperature component of the response. The electrical parameters of film 2 to which a strong magnetic field (of the order of several tens of tesla) was applied were similar to those observed for $I_b\geqslant10$ mA in zero magnetic field.

Afanasyev *et al.*[79,80] concluded that the monitoring mechanism for epitaxial films is either purely bolometric, or is associated with electron heating,[76] while the model of a two-dimensional ($2D$) network of disordered granules connected through weak links with a wide spread of critical currents I_{ci} is more appropriate for granular films. According to Likharev,[60] the energy $E_{ci}=hI_{ci}/4\pi e$ of the ith link at $T\sim T_c$ is comparable with the thermal energy k_BT, and hence the weak link has a finite resistance $R_i=R_{Ni}F(E_{ci}/k_BT)$, where $F(z)\sim\exp(-2z)$ in the case of weak links with strong attenuation in the limit $z\gg1$. The calculation of electrical characteristics of the film is reduced to determining the resistance of the random network of weak links with an exponential spread of resistance.[81] In this case, R is equal to the resistance $R_m=R_{N_m}F(z_m)$ of the weakest link with highest resistance in cluster formed by weak links with $R_i\leqslant R_m$ to within the pre-exponential factor $(E_c/k_BT)^{\tilde{\nu}}$ ($\tilde{\nu}$ is the critical index of correlation length). Here the resistance R_{N_m} is equal to the resistance R_N of an ensemble of weak links in the normal state to within the coefficient of the order of unity. The response of a superconductor in such a system is determined by the variation of I_c under irradiation, i.e.,

$$\Delta V=I\Delta R\simeq I\Delta I_cR_{N_m}\frac{dF}{dI_c}\sim z_m\exp(-2z_m), \tag{29}$$

where $z_m=-hI_b/4\pi ek_BT$, and I_{cm} is the critical current of the mth weak link.[79] Expression (29) shows that the resistance as well as the response of a granular film must decrease exponentially in the region of resistive tail, which was actually observed in experiments.[78] According to this model, the response must have a peak at $z\simeq1$, which corresponds to a temperature T defined by the equation

$$T_c-T=2\pi T_c\overline{R}_Ne^2/h. \tag{30}$$

It follows hence that as the film quality improves (as I_c increases and $\overline{R}_N$ decreases), the low-temperature peak must be shifted to T_c, which was also confirmed in experiments.[78] When the value of I_c is high and comparable with the value of I_c of granules, the bolometric mechanism or electron heating become dominating, and the peak of the response in this case coincides with the dR/dT peak. The responsivity of the low-temperature component was 10^2–10^3 V/W in the temperature range 20–60 K, while that for the bolometric re-

sponse was smaller than 10^2 V/W. These values of responsivity were obtained for a film in the resistive state with a resistance of 1 Ω. These results are compared with the monitoring mechanism observed by Bertin and Rose[82] who studied the films of tin molten into the gold matrix, creating an artificial granular structure. Bertin and Rose[82] emphasized that the *enhanced monitoring* conditions observed by them is typical only of films with a high resistance R_n in the normal state ($\sim$11.4 kΩ). These conditions exist along with the bolometric mode, but differ significantly from the latter in a stronger response. It was assumed that this is a result of a nonlinear response to currents induced in the film by incident EMR.

Finally, according to the percolation model 78, the current flows only through a few channels formed by weak links with the lowest resistance in view of strong spatial inhomogeneity of films. These channels are combined into clusters with a certain characteristic correlation length which is in fact equal to the separation between these clusters. Such a pattern was confirmed by laser probing of the film. The dependence of variation of the voltage across the field due to weak local heating by radiation ($\Delta T \ll T_c$) on the coordinate along the film had the form of nearly periodic peaks having different amplitudes (obviously, due to different resistances of various regions of a cluster) with a characteristic period ~ 100 μm. This value is just the correlation length of the cluster being formed.

Salient features and conditions for realization of the mechanism

(1) The presence of a low-temperature component of the response in the region of resistive tail, which increases in amplitude and which is shifted towards low temperatures upon an increase in I_b and to T_c as a result of improvement of the film quality.
(2) An exponential decrease of the response as well as dc resistance upon cooling.
(3) The presence of a peak at the temperature determined by the relation $hI_{\rm cm}/4\pi e k_B T = 1$.
(4) The high value of responsivity ($\sim 10^2 - 10^3$ V/W) which increases with the film resistance in the normal state.

2.8. Stimulation of superconductivity

An increase in the critical current in thin superconducting bridges induced by EMR was observed for the first time Wyatt *et al.*[83] This was followed by a number of works devoted to this problem (see the review by Dmitriev and Khristenko in Ref. 67). Since stimulation of superconductivity was detected below as well as above T_c, it is often referred to as the effect of stimulation and induction of superconductivity by EMR. For a long time, the effect of stimulation was observed only in weakly coupled superconductors, and was detected much later in narrow, thin, and long films (see Ref. 8 in the literature cited by Dmitriev and Khristenko[67]). Manifestations of the effect in weakly coupled structures and in long homogeneous channels are quite similar, although their mechanisms are different. Besides, the stimulation of superconductivity in bridges is limited by the effective volume of the weak link, while in long channels it is limited by the structure width. The most significant difference between the stimulation in bridges and in long channels is that the superconducting transition temperature and the critical current in the bridge do not exceed corresponding values for the banks. On the contrary, the critical current $I_c(P_\omega)$ in long films exposed to radiation is noticeably larger than the Ginzburg–Landau depairing current. It is appropriate to consider a new state in the MW field with a new energy distribution function for electrons and with the gap $\Delta(P_\omega)$ in the energy spectrum, whose width is larger than that of the unperturbed gap $\Delta(0)$. Long narrow films as well as bridges are characterized by the lower (ω_1) and upper (ω_2) boundary frequencies of the effect. The two boundary frequencies increase upon cooling.

The stimulation effect was initially explained on the basis of phenomenological models (Refs. 5 and 15–18 in the literature cited in Ref. 67) which described its salient features, but failed to explain some peculiarities of the effect (such as the presence of the upper and lower frequency boundaries of the effect, different manifestations of the effect in weakly coupled structures and in long homogeneous superconducting channels, and the coexistence of the Josephson effect with the effect of stimulation and induction of superconductivity in weakly coupled superconductors). The Eliashberg microscopic theory[66] and the Aslamazov–Larkin theory[84] which appeared later described superconductivity stimulation in homogeneous superconductors and in heterogeneous weakly coupled junctions, respectively.

The Eliashberg microscopic theory[66] is based on the assumption that radiation of frequency $\nu < 2\Delta/h$ does not change the total number of excitations in a superconductor, but can lead to a displacement of the ''center of gravity'' of the electron distribution function $f(\varepsilon)$ towards higher energies due to absorption of the MW energy by excitations located near the edge of the gap. According to the basic equation of the BCS theory connecting the energy gap Δ with the electron distribution function $f(\varepsilon)$, this must lead to an increase in Δ, and hence to the enhancement of superconducting properties of the sample.[66]

According to the Aslamazov–Larkin theory,[84] the order parameter Δ in the contact region of heterogeneous junctions carrying a direct current becomes smaller than the order parameter Δ_0 in the banks outside this region. The electrons with energy $\varepsilon < \Delta_0$ become ''trapped'' in the contact and move within the potential well, being reflected by its walls. The application of an ac field causes ''quivering'' of the potential well, and hence to energy diffusion of electrons. As a result, the electron distribution function becomes nonequilibrium, the deviation from equilibrium being most significant at the center of the junction, where the number of electrons decreases as compared to the equilibrium case due to energy diffusion. This is equivalent to effective cooling of the junction. At the same time, electron diffusion may cause the accumulation of electrons in the region of high energies leading to heating of the junction. The resultant effect depends on the radiation power.

The stimulation of superconductivity in HTSC materials by MW radiation was also observed, but it was studied less

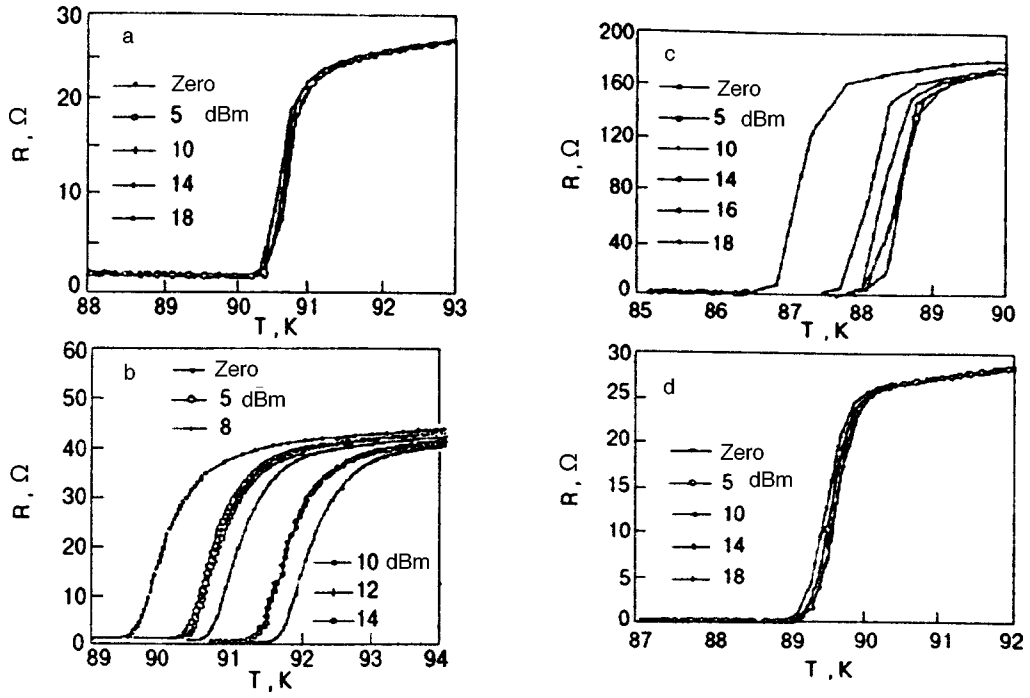

FIG. 24. The $R(T)$ dependence enhanced by microwave radiation for $\theta=24°$ (a), 36.8° (b), and 45° (c). The results for intragranular boundary of a bridge with $\theta=36.8°$ are shown for comparison (d). It can be seen that stimulation is significant for weakly coupled junctions (from Fu *et al.*[86]).

comprehensively than in traditional superconductors. This can be explained, above all, by small number of publications in this field, which is due to some peculiarities of new superconductors. For example, the small value of ξ complicates the preparation of weak links with parameters satisfying the conditions limiting the sample size, which must be satisfied to observe stimulation according to the Aslamazov–Larkin mechanism, while the strong electron–electron interaction associated with the small mean free path l hampers the superconductivity stimulation according to the Eliashberg mechanism.[66,67]

First communications concerning the superconductivity stimulation in HTS samples by MW radiation[85] were purely ''speculative'' and did not lay claims on a detailed description of the observed effect or its analysis. Later, Dmitriev *et al.*[44] reported the observation of nonequilibrium effects in YBaCuO ceramic bridges. Among other things, they observed stimulated excess current in the bridges exposed to MW signal at frequency 13.3 GHz. It was proved that in spite of the emergence of Shapiro steps on IVC as a result of irradiation by MW signal, the dependence of I_c on $P_\omega^{1/2}$ cannot be described by a Bessel function as expected for bridges. On the contrary, this curve consists of two linear regions typical of a long superconducting channel. Dmitriev *et al.*[44] also observed that the passage of direct current for radiation powers higher then the critical value $P_\omega^c(I_c(P_\omega^c)=0)$ leads to a transition from the normal to the resistive state. The transition current I_{tr} increases with the MW power. This effect was observed in HTSC materials for the first time and was attributed to a charge redistribution between ''active'' CuO_2 planes and the ''reservoir'' of chains, which is induced by the direct current. This can lead to an increase in the number density of holes in CuO_2 planes, where the holes form pairs. Detailed measurements and an analysis of the results as well as a comparison with available data for low-temperature superconductor led Dmitriev *et al.*[44] to the conclusion that the stimulation of superconductivity in YBaCuO ceramic bridges occurs according to the Aslamazov–Larkin mechanism due to energy diffusion of electrons localized in the constriction region.

Fu *et al.*[86] studied the response of bridges made of YBaCuO epitaxial films on $SrTiO_3$ bicrystalline substrates to MW radiation ($\nu=12.4$ GHz). The typical size of the bridges was 60 μm×20 μm×120 nm. The response of the intragranular as well as intergranular regions was measured simultaneously by using the four-probe technique. The obtained $R(T)$ dependence shows that the normal resistance in a sample region which does not intersect a weak link is an order of magnitude lower, and the transition width is much smaller than the corresponding values for a region intersecting a weak link. Besides, the measurements of IVC for a region intersecting a weak link revealed the presence of steps satisfying the Josephson relation. Fu *et al.* came to the conclusion that the blurring of the transition for a region with a weak link is associated with the formation of PSC.

An analysis of the $R(T)$ dependences for three different disorientation angles θ for the bicrystalline substrate proved that MW power virtually does not affect $R(T)$ for $\theta=24°$, while the value of T_c increases with radiation power for $\theta=36°$ and 45° (Fig. 24). The maximum effect was observed for $\theta=45°$. Since the entire superconducting transition was shifted by 2–3 K above the equilibrium value of T_c, and the value of T_c increases only for the region of weak link, Fu *et al.*[86] believe that the observed phenomenon may be due not only to fluctuations or effects of redistribution of nonequilibrium quasiparticles. It is proposed that stimulation fol-

lowing the Aslamazov–Larkin mechanism takes place in the given case. The measurements of the $I_c(T)$ dependence for weak links with different disorientation angles θ for substrate crystals revealed that it has the form $I_c \sim (1-T/T_c)^2$ typical of weak links of the SNS type for all three junctions. However, a departure (''bend'') from the theoretical dependence is observed for $\theta = 24°$ in a narrow range of low temperatures. Fu *et al.*[86] believe that this confirms the existence of a stronger intergranular coupling inherent in this junction and assume that the difference in the transport properties of the three boundary weak links is due to their geometrical structure; the differences in these structures are also manifested in the $R(T)$ dependences for different values of P_ω (see Fig. 24).

Choudhury *et al.*[87] studied the MW surface impedance of a suspended strip of YBaCuO epitaxial film in a constant magnetic field up to 1000 Oe. The MW magnetic field was parallel to the (ab) plane of the sample, while the constant field was applied along the **c**-axis. It was found that a weak magnetic field (of the order of several oersteds) leads to a decrease in R_s. The maximum effect ($\sim 20\%$) was observed in a field of 5 Oe. while superconductivity suppression (increase in R_s) was observed in a field above 25 Oe. The measurements of the $R_s(H)$ dependence upon sweeping of H from -100 to $+100$ Oe revealed that a hysteresis of the MW response (i.e., the lack of coincidence in the shape of the magnetic-field dependence with the initial curve upon repeated field sweeping) appears even for low radiation powers (by 21 dB·m below 1 mW). It was concluded[87] that the MW field competes with the constant field, leading to the emergence of vortices in the sample, which are subsequently entangled with lattice defects (pinning). It was proposed that the observed decrease in R_s is due to nonequilibrium redistribution of quasiparticles, which is induced by MW radiation and leads to superconductivity stimulation in the presence of direct current I_{dc}. It was also emphasized that since HTSC materials exhibit a nonmonotonic dependence $R_s(T)$ $(dR_s/dT<0)$, the manifestation of the effect for which $dR_s/dI_{dc}<0$ is not surprising.

Salient features and conditions for the realization of the mechanism

(1) Superconductivity simulation is observed in heterogeneous and long homogeneous superconducting channels and is manifested experimentally in an increase in superconducting transition temperature and critical current and a decrease in the dc or ac resistance. In bridges and other types of spatially inhomogeneous weak links, the stimulation follows the Aslamazov–Larkin mechanism, while in long and narrow channels it is governed by the Eliashberg mechanism.
(2) Both mechanisms are characterized by the existence of the lower and upper boundaries of the effect, the corresponding frequencies increasing upon cooling.
(3) The decisive role in the emergence of the effect in heterogeneous junctions is played by their volume (which must be smaller than a certain value), while for narrow homogeneous channels the leading role is played by their width (which must satisfy the same requirement).
(4) The main difference between superconductivity stimulation in bridges and in long homogeneous channels is that the critical temperature (or critical current) of the former never exceed the same for the ''banks,'' while the critical current for the channels can not only be larger than the value of I_c in the absence of radiation, but can even exceed the equilibrium depairing current.

CONCLUSIONS

Thus, bolometric and nonbolometric mechanisms can obviously be realized in HTSC materials of any quality. The main nonequilibrium mechanism for granular samples exposed to radiation at frequencies $\nu \ll 2\Delta/h$ is the inverse transient Josephson effect for which the peak of the response lies in the region of resistive ''tail'' of the temperature dependence of resistance and is separated by a considerable temperature interval from the peak of the bolometric response. As the sample quality is improved, the peaks of the nonbolometric and bolometric responses become closer and almost coincide for high-quality epitaxial films. The prevailing mechanisms of the nonequilibrium response are either the radiation-induced flow of magnetic flux trapped in weak links or in granules (in the presence of a strong constant magnetic field), or the phase slip at intergranular weak links and Josephson junctions formed by overlapping segments of adjacent copper-oxygen planes. In spite of the fact that the peaks of the response of the above-mentioned ''high-temperature'' mechanisms almost coincide on the temperature scale with the peaks of the bolometric component, they can be analyzed by using contactless methods of recording (which do not lead to strong nonlinear effects and heating due to a large contact resistance), and the incident radiation with a frequency $\gtrsim 10$ kHz can be modulated in order to eliminate the bolometric effect.

At radiation frequencies $\nu > 2\Delta/h$, electron heating and nonequilibrium variation of kinetic inductance are the dominating nonthermal mechanisms over virtually the entire temperature range below T_c. The fundamental parameters typical of these mechanisms can be observed by monitoring the response by the ''pump–probe'' method in which the signal from the same source (laser) is used to act on the sample and to measure the response (after attenuation and delay). This method is rather effective in the case of short (<1 ps) radiation pulses which do not impose limitations on characteristic times of the response of the picosecond scale. The only drawbacks of the ''pump–probe'' method are its technical complexity and the high cost of the precision instruments. For this reason, monitoring with RF or MW displacement as a simpler economical method can be considered an alternative. However, limitations on the response times as well as the inertia of RF monitoring technique must be determined beforehand.

The authors express their gratitude to Prof. V. M. Dmitriev for valuable remarks made while reading the preliminary version of this review. Thanks are also due to M. A. Hein, P. G. Huggard, W. M. Huber, M. Lindgren, D. P. Choudhury, C. M. Fu, Yu. P. Gusev, and A. M. Kadin who

presented copies of their published and unpublished papers.

*E-mail: velichko@ire.kharkov.ua

[1] G. Blatter, M. V. Feigel'man, V. B. Geshkenbein *et al.*, Rev. Mod. Phys. **66**, 1125 (1994).
[2] M. A. Hein, *Studies of High-Temperature Superconductors*, Nova Science Publ., New York (1996).
[3] Gi. Schneider, P. G. Huggard, T. P. O'Bien, and W. Blau, Solid State Commun. **89**, 705 (1994).
[4] P. L. Richards, J. Clarke, R. Leoni *et al.*, J. Appl. Phys. **54**, 283 (1989): J. Clarke, G. I. Hoffer, P. L. Richards, and N. H. Yeh, J. Appl. Phys. **48**, 4865 (1977).
[5] M. Lindgren, M. Currie, C. Williams *et al.*, in *Proc. of ASC'96, ER- 4*.
[6] M. Lindgren, M. Currie, C. Williams *et al.*, J. of Selected Topics in Quantum Electronics **2**, 668 (1996).
[7] G. N. Gol'tsman, P. Kouminov, I. Goghidze, and E. M. Gershenson, IEEE Trans. Appl. Supercond. **5**, 2591 (1995).
[8] M. A. Heusinger, A. D. Semenov, R. S. Nebosis *et al.*, IEEE Trans. Appl. Supercond. **5**, 2595 (1995).
[9] M. W. Johnson, A. M. Domino, and A. M. Kadin, J. Appl. Phys. **79**, 7069 (1996).
[10] M. Leung, P. P. Broussard, J. H. Claassen *et al.*, Appl. Phys. Lett. **50**, 2046 (1987).
[11] N. T. Cherpak, E. V. Izhyk, A. Ya. Kirichenko *et al.*, in *Int. Conf. on HTSC and Localization Phenomena*, Moscow (1991); A. V. Velichko, E. V. Izhyk, A. Ya. Kirichenko *et al.*, in *1st Ukrainian Symp. on Physics and Engineering of mm and submm Waves*, Kharkov (1991); A. V. Velichko, N. T. Cherpak, E. V. Izhyk *et al.*, in *Proc. Int. Symp. on Physics and Engineering of mm and submm Waves*, Kharkov (1994).
[12] A. L. Dorofeev, *Induction Spectroscopy* [in Russian], Energiya, Moscow (1973).
[13] F. F. Mende, I. N. Bondarenko, and A. V. Trubitsyn, *Superconducting and Cooled Resonant Systems* [in Russian], Naukova Dumka, Kiev (1978).
[14] S. G. Han, Z. V. Vardeny, K. S. Wong, and O. G. Symko, Phys. Rev. Lett. **65**, 2708 (1990).
[15] R. Sobolewski, L. Shi, T. Gong *et al.*, Proc. SPIE **2159**, 110 (1990).
[16] P. W. Anderson, Phys. Rev. Lett. **9**, 309 (1962).
[17] E. Zeldov, N. M. Amer, G. Koren, and A. Gupta, Phys. Rev. B **39**, 9712 (1989).
[18] A. Frenkel, E. Clausen, C. C. Chang *et al.*, Appl. Phys. Lett. **55**, 911 (1989); A. Frenkel and C. C. Chang, J. Mater. Res. **5**, 691 (1990).
[19] A. Frenkel, Physica C **180**, 251 (1991).
[20] W. Eideloth, IEEE Trans. Magn. **27**, 2828 (1991).
[21] T. T. M. Palstra, B. Batlogg, R. B. van Dover *et al.*, Phys. Rev. B **41**, 6621 (1990).
[22] M. Tinkham, Phys. Rev. Lett. **61**, 1658 (1988).
[23] V. Ambegaokar and B. J. Halperin, Phys. Rev. Lett. **22**, 1364 (1969).
[24] Y. Yeshurun and P. A. Malozemoff, Phys. Rev. Lett. **60**, 2202 (1988).
[25] M. P. A. Fisher, Phys. Rev. Lett. **62**, 1415 (1989).
[26] P. H. Kes, J. Aarts, J. van der Berg *et al.*, Supercond. Sci. Technol. **1**, 242 (1989).
[27] J. Bardeen and M. J. Stephen, Phys. Rev. A **140**, 1197 (1965).
[28] L. Ji, M. S. Rzchowski, and M. Tinkham, Phys. Rev. B **42**, 4838 (1990).
[29] A. M. Portis, K. W. Blazey, K. A. Müller, and J. G. Bednordz, Europhys. Lett. **5**, 467 (1988).
[30] A. V. Velichko, Ph.D thesis, Kharkov (1996).
[31] Yu. V. Medvedev and A. S. Petrov, Izv. Vuzov. Fizika **10**, 93 (1972); I. I. Eldumiatti and G. A. Haddad, IEEE Trans. Electron Devices **19**, 257 (1972).
[32] A. V. Velichko, N. T. Cherpak, E. V. Izhyk *et al.*, Physica C **261**, 220 (1996); A. V. Velichko, N. T. Cherpak, E. V. Izhyk *et al.*, Physica C **277**, 101 (1997).
[33] A. V. Velichko, N. T. Cherpak, E. V. Izhyk *et al.*, Fiz. Nizk. Temp. **22**, 963 (1996) [Low Temp. Phys. **22**, 533 (1996)]; A. V. Velichko, N. T. Cherpak, E. V. Izhyk *et al.*, Czech. J. Phys. **46**, 1639 (1996).
[34] A. Gurevich and H. Küpfer, Phys. Rev. B **48**, 6477 (1993).
[35] J. Halbritter, J. Appl. Phys. **68**, 6315 (1990).
[36] S. Sridhar, Appl. Phys. Lett. **65**, 1054 (1994).
[37] A. Gurevich, Physica C **243**, 191 (1995).
[38] I. M. Dmitrenko, Fiz. Nizk. Temp. **22**, 849 (1996) [Low Temp. Phys. **22**, 648 (1996)].
[39] V. V. Shmidt, *Introduction to Superconductor Physics* [in Russian], Nauka, Moscow (1982).
[40] H. A. Blackstead, D. B. Pulling, P. J. McGinn, and J. Z. Liu, Physica C **174**, 394 (1991).
[41] W. K. Kwok, U. Welp, G. W. Crabtree *et al.*, Phys. Rev. Lett. **64**, 966 (1990).
[42] J. M. Kosterlitz and D. J. Thouless, J. Phys. C **6**, 1181 (1973).
[43] H. A. Blackstead, J. Supercond. **5**, 67 (1992).
[44] V. M. Dmitriev, I. V. Zolochevskii, and E. V. Khristenko, Fiz. Nizk. Temp. **19**, 249 (1993) [Low Temp. Phys. **19**, 173 (1993)].
[45] J. C. Culbertson, U. Strom, S. A. Wolf *et al.*, Phys. Rev. B **39**, 12359 (1989); A. T. Fiory, A. F. Hebard, P. M. Manikiewich, and R. E. Howard, Phys. Rev. Lett. **61**, 1419 (1988).
[46] A. M. Kadin, M. Leung, and A. D. Smith, Phys. Rev. Lett. **65**, 3162 (1990).
[47] A. M. Kadin, M. Leung, A. D. Smith, and J. M. Murduck, IEEE Trans. Magn. **27**, 1540 (1991).
[48] W. J. Skocpol, M. R. Beasley, and M. Tinkham, J. Low Temp. Phys. **16**, 145 (1974).
[49] A. M. Kadin, M. Leung, A. D. Smith, and J. M. Murduck, Appl. Phys. Lett. **57**, 2847 (1990).
[50] M. W. Johnson, A. M. Domino, and A. M. Kadin, IEEE Trans. Appl. Supercond. **5**, 2587 (1995).
[51] W. J. Skocpol, M. R. Beasley, and M. Tinkham, J. Appl. Phys. **45**, 4054 (1974).
[52] D. N. Langerberg, D. J. Scalapino, B. N. Taylor, and R. E. Eck, Phys. Lett. **20**, 563 (1966).
[53] R. Durny, S. Ducharme, J. Hautala *et al.*, Physica C **162–164**, 1065 (1989).
[54] K. Chang, J. T. Chen, and L. E. Wenger, Physica C **162–164**, 1591 (1989); K. Chang, G. Yong, L. E. Wenger, and J. T. Chen, Appl. Phys. Lett. **59**, 7316 (1991).
[55] J. C. Gallop, W. J. Radcliffe, C. D. Langhman *et al.*, Physica C **162–164**, 1545 (1989).
[56] B. G. Boone, R. M. Sova, K. Moorjani, and W. J. Green, Appl. Phys. Lett. **59**, 2676 (1991).
[57] P. G. Huggard, Gi. Schneider, T. P. O'Brien *et al.*, Appl. Phys. Lett. **58**, 2549 (1991).
[58] P. Russer, J. Appl. Phys. **43**, 2008 (1972).
[59] A. Barone and G. Patterno, *Physics and Application of the Josephson Effect*, Wiley, New York (1986).
[60] K. K. Likharev, *Introduction to the Dynamics of Josephson Junctions* [in Russian], Nauka, Moscow (1985).
[61] Gi. Schneider, P. G. Huggard, T. P. O'Brien *et al.*, Appl. Phys. Lett. **60**, 648 (1992).
[62] L. Ngo Phong and T. Shin, J. Appl. Phys. **74**, 7414 (1993).
[63] A. Irie and G. Oya, IEEE Trans. Appl. Supercond. **5**, 3267 (1995).
[64] D. C. Ling, J. T. Chen, and L. E. Wenger, Phys. Rev. B **53**, 1 (1996).
[65] A. Gilabert, Ann. Phys. (Paris) **15**, 255 (1990).
[66] G. M. Eliashberg, Pis'ma Zh. Éksp. Teor. Fiz. **11**, 186 (1970) [JETP Lett. **11**, 114 (1970)].
[67] V. M. Dmitriev and E. V. Khristenko, Fiz. Nizk. Temp. **4**, 821 (1978) [Sov. J. Low Temp. Phys. **4**, 387 (1978)].
[68] Y. Enomoto, T. Murakami, and M. Suzuki, Physica **B** and C **148**, 408 (1988); Y. Enomoto and T. Murakami, Jpn. J. Electr. Commun. Lab. Tech. **34**, 1597 (1985); M. Suzuki, Y. Enomoto, and T. Murakami, J. Appl. Phys. **56**, 2083 (1984).
[69] H. Tanabe, Y. Enomoto, M. Suzuki *et al.*, Jpn. J. Appl. Phys., Suppl. **29**, L466 (1990).
[70] M. Johnson, Appl. Phys. Lett. **59**, 1371 (1991).
[71] A. D. Semenov, G. N. Gol'tsman, J. G. Gogidze *et al.*, Appl. Phys. Lett. **60**, 903 (1992); N. Bluzzer, Phys. Rev. B **46**, 1033 (1992).
[72] Z. M. Zhang and A. Frenkel, J. Supercond. **7**, 871 (1994).
[73] S. G. Han, Z. V. Vardeny, O. G. Symko, and G. Koren, IEEE Trans. Magn. **27**, 1548 (1991).
[74] S. I. Anisimov, B. L. Kapeliovich, and T. L. Perel'man, Zh. Éksp. Teor. Fiz. **66**, 776 (1974); T. Q. Qiu and C. L. Tien, Int. J. Heat Mass Transf. **35**, 719 (1992).
[75] A. Frenkel, Phys. Rev. B **48**, 9717 (1993).
[76] É. M. Gershenson, M. E. Gershenson, G. N. Gol'tsman *et al.*, Pis'ma Zh. Éksp. Teor. Fiz. **34**, 281 (1981) [JETP Lett. **34**, 268 (1981)]; E. M. Gershenson, M. E. Gershenson, G. N. Gol'tsman *et al.*, Zh. Éksp. Teor. Fiz. **86**, 758 (1984) [Sov. Phys. JETP **59**, 442 (1984)]; E. M. Gershenson, M.

E. Gershenson, G. N. Gol'tsman *et al.*, IEEE Trans. Magn. **27**, 2836 (1991).
[77] È. E. Aksaev, E. M. Gershenzon, G. N. Gol'tsman *et al.*, Sverkhprovodimost': Fiz., Khim., Tekh. **3**, 1933 (1990).
[78] A. S. Afanasyev, V. N. Gubankov, P. M. Shadrin, and A. F. Volkov, in *Proc. of ISEC*, Tokyo (1989).
[79] A. S. Afanasyev, A. F. Volkov, V. N. Gubankov *et al.*, IEEE Trans. Magn. **25**, 2571 (1989).
[80] A. S. Afanasyev, A. F. Volkov, and V. N. Gubankov, Fiz. Nizk. Temp. **15**, 322 (1989) [Sov. J. Low Temp. Phys. **15**, 181 (1989)].
[81] B. I. Shklovskii, *Electronic Properties of Doped Semiconductors*, Springer-Verlag, New York, NY (1984).
[82] C. L. Bertin and K. Rose, J. Appl. Phys. **42**, 631 (1971).
[83] A. F. G. Wyatt, V. M. Dmitriev, V. M. Moore, and F. W. Sheard, Phys. Rev. Lett. **16**, 1166 (1966).
[84] L. G. Aslamazov and A. I. Larkin, Zh. Éksp. Teor. Fiz. **74**, 2184 (1978) [Sov. Phys. JETP **47**, 1136 (1978)].
[85] E. M. Rudenko, I. V. Korotash, I. P. Neverkovets *et al.*, Supercond. Sci. Technol. **4**, 1 (1991); A. Ya. Kirichenko, M. B. Kosmyna, A. B. Levin, and N. T. Cherpak, Pis'ma Zh. Éksp. Teor. Fiz. **50**, 260 (1989) [JETP Lett. **50**, 260 (1989)].
[86] C. M. Fu, J. Y. Juang, M. F. Chen *et al.*, IEEE Trans. Appl. Supercond. **5**, 2196 (1994).
[87] D. P. Choudry, B. A. Willemsen, J. S. Derov, and S. Sridhar, IEEE Trans. Appl. Supercond. **7**, 1260 (1996).

Translated by R. S. Wadhwa